NACA TN 2840

NATIONAL ADVISORY COMMITTEE
FOR AERONAUTICS

TECHNICAL NOTE 2840

BUCKLING OF LOW ARCHES OR CURVED BEAMS

OF SMALL CURVATURE

By Y. C. Fung and A. Kaplan

California Institute of Technology

NACA

Washington

November 1952

NATIONAL ADVISORY COMMITTEE FOR AERONAUTICS

TECHNICAL NOTE 2840

BUCKLING OF LOW ARCHES OR CURVED BEAMS

OF SMALL CURVATURE

By Y. C. Fung and A. Kaplan

SUMMARY

When a low arch (a thin curved beam of small curvature) is subjected
to a lateral loading acting toward the center of curvature, the axial
thrust induced by the bending of the arch may cause the arch to buckle
so that the curvature becomes suddenly reversed. The critical lateral
loading depends on the dimensions and rigidity of the arch, the elasticity
of the end fixation, the type of load distribution, and the initial
curvature of the arch. A general solution of the problem is given in
this paper, using the classical buckling criterion which is based on the
stability with respect to infinitesimal displacements about the equilib-
rium positions.

For a sinusoidal arch under sinusoidal loading, the critical load
can be expressed exactly as a simple function of the beam dimension
parameters. For other arch shapes and load distributions, approximate
values of the critical load can be obtained by summing a few terms of
a rapidly converging Fourier series. The effects of initial end thrust
and axial and lateral elastic support are discussed.

The buckling load based on the energy criterion of Kármán and Tsien
is also calculated. The results for both the classical and the energy
criteria are compared with experiments made on a series of centrally
loaded, pin-ended arches. For larger values of a dimensionless param-
eter λ_1, which is proportional to the ratio of the arch rise to the
arch thickness, the experimental critical buckling loads agreed quite
well with the classical criterion, but, for smaller values of λ_1, the
experimental critical loads were appreciably below those calculated from
the classical criterion, although they were always above those obtained
from the energy criterion.

INTRODUCTION

An arch subjected to lateral loads may become elastically unstable.
Generally speaking, there are two possibilities of buckling:

(1) If the rise of the arch (a in fig. 1) is of the same order as the span of the arch, then it is possible for the arch to buckle at the critical pressure in the mode indicated by the dashed curve in figure 1. Buckling of this type can be safely assumed to be "inextensional," as suggested by Lord Rayleigh, and, as such, has been discussed by E. Hurlbrink, E. Chwalla, R. Mayer, E. Gaber, E. L. Nicolai, and S. Timoshenko. (See Timoshenko's book, reference 1, for references to original papers.) In all these studies, circular arches under uniformly distributed lateral loading are assumed, with various types of end fixations.

(2) If the rise a of the arch is much smaller than the span L, (fig. 2), then the induced axial thrust plays an important role in the elastic stability. The beam may become unstable and suddenly reverse its curvature, jumping, for example, from the solid-line position in figure 2 to the dashed-line position.

It is the object of the present paper to treat arches of small rise; therefore, the buckling deformation will be "extensional" rather than "inextensional." It will be shown that the variation in the initial curvature of the beam has a very important effect on the critical load. Furthermore, with a view to possible applications to thin-wing design problems, beams acted on by initial thrust and those with elastic supports will be discussed.

The same problem has been treated before by Biezeno (reference 2), Marguerre (references 3 and 4), Timoshenko (reference 1), and Friedrichs (reference 5).[1] Biezeno and Timoshenko derived the fundamental differential equation in the same manner as this paper, while Marguerre and Friedrichs derived their equations by variational principles. The resulting equations are the same. Biezeno treated a circular arch under a concentrated load at the center and Marguerre and Friedrichs, a circular arch under uniformly distributed pressure; all arrived at the main features of the buckling problem, but the calculations are rather involved. Timoshenko assumed that the center line of the deflected beam as well as the initial shape is a half wave of a sine curve and arrived at a very simple solution. The restriction of the buckling mode to the symmetrical one, however, sometimes gives the critical buckling load manyfold too high in a certain range of arch rise.

The buckling criterion used by the authors of references 1 to 5 is the classical one which is based on the stability with respect to

---

[1]After completion of the present work, it was learned that Hoff and Bruce (reference 6) treated a similar problem from the point of view of dynamic stability. Part of Hoff and Bruce's work coincides almost identically with the present report.

infinitesimal displacements about the equilibrium positions. But
Friedrichs, in reference 5, also calculated the buckling load on the
basis of Tsien's energy criterion, which is based on finite displace-
ments. The energy criterion yields a buckling load much lower than
that obtained from the classical criterion. It is not evident which
of these two criteria corresponds to the real practical situation.
Therefore in this paper, both criteria will be used and the results
will be compared with experiments.

This work was conducted at the California Institute of Technology
under the sponsorship and with the financial assistance of the National
Advisory Committee for Aeronautics.

SYMBOLS

A cross-sectional area of beam

a rise of arch

E Young's modulus

F dead-weight load (in section "Buckling Load Based on Kármán
           and Tsien's Energy Criterion")

H axial compression at ends of beam

H_o initial thrust in beam

I moment of inertia (or second moment) of cross section of beam

$K = \pi^4 EI^2 / AL^3$

$$k = \frac{1}{36}\left[\frac{\lambda_1 + \sqrt{\frac{4}{27}\left(\lambda_1^2 - 1 - k\right)^3}}{\lambda_1^2 - 13}\right]^2$$

L span of beam

M bending moment; positive when it tends to put upper side of
           beam in compression

M_o bending moment due to lateral forces alone

Q   shearing force in beam; positive when $\displaystyle\int_{\Delta x} Q\,dx$ produces

     positive moment

q   lateral pressure per unit length of beam; positive downward
     (in negative y-direction)

q_o characteristic lateral pressure per unit length of beam

t   thickness of beam

U   strain energy

V   change in thrust in lateral support

W   total load beam can sustain without buckling

$y,\ y_o$ actual and initial curve of center line of beam, respectively

α spring constant of arch support

α' spring constant of lateral support

Δ distance spring-supported end of beam is displaced

δ deviation ratio $\left(a_m/a_l\right)$

ρ_o radius of circular-arc arch

σ_b bending stress in beam

σ_c axial stress in beam

$\sigma_p = \left(\pi^2 EI/L^2\right)\big/ A$

ϕ total energy for dead-weight loading

Subscripts:

class   classical criterion

conc   concentrated loading

cr   critical

energy   energy criterion

exp   experimental

max   maximum

sine   sinusoidal loading

unif   uniform loading

Nondimensional coefficients:

Let

$$y_o = \sum_{m=1}^{\infty} a_m L \sin \frac{m\pi x}{L}$$

$$y = \sum_{m=1}^{\infty} b_m L \sin \frac{m\pi x}{L}$$

$$q = q_o f(x)$$

Then

$$\lambda_m = \frac{a_m L}{2} \sqrt{\frac{A}{I}} \qquad\qquad (m = 1, 2, 3, \ldots)$$

$$B_m = \frac{b_m L}{2} \sqrt{\frac{A}{I}} \qquad\qquad (m = 1, 2, 3, \ldots)$$

$$R = \frac{q_o L^4}{2\pi^4 EI} \sqrt{\frac{A}{I}}$$

$$S = \frac{H_o L^2}{\pi^2 EI}$$

$$\beta = \frac{\alpha}{\alpha + \dfrac{EA}{L}}$$

$$\mu = \frac{2\alpha' L^3}{\pi^4 EI}$$

GENERAL ANALYSIS

Consider a thin curved beam of small curvature, one end of which is hinged, that is, it is free to rotate but is fixed in position, while the other end of the beam is attached to a spring, with a spring constant α. When the spring-supported end is displaced by a distance Δ, the thrust induced in the spring will be

$$H = H_o + \alpha\Delta \tag{1}$$

where H_o is the initial thrust built in the beam.[2] (See fig. 3.) Before the application of the lateral load $q(x)$, the axial load in the beam is H_o and the beam center line is represented by the following Fourier series:

$$y_o = \sum_{m=1}^{\infty} a_m L \sin \frac{m\pi x}{L} \tag{2}$$

Under the lateral load q, the displaced center line can be written as

$$y = \sum_{m=1}^{\infty} b_m L \sin \frac{m\pi x}{L} \tag{3}$$

Assume that $|y_o|$ and $|y|$ are much smaller than L, and hence $|a_m|$ and $|b_m|$ are much smaller than 1; that the beam is made of homogeneous material, of constant cross section, and with small curvature so that $(dy/dx)^2$ is negligible in comparison with 1; and that the thickness of the beam is much smaller than the radius of curvature of the beam. Then the usual beam theory gives

$$EI\left(\frac{d^2y}{dx^2} - \frac{d^2y_o}{dx^2}\right) = M \tag{4}$$

---

[2]No generality is lost by treating this case of one end spring instead of the case with both ends of the beam elastically supported because the springs at both ends can be replaced by a single spring at one end.

where M is the increase in bending moment due to the application of $q(x)$. From statics,

$$M = \int_0^x Q \, dx - (Hy - H_0 y_0) \tag{5}$$

Substituting equation (5) into equation (4) and differentiating twice, remembering that $\frac{dQ}{dx} = -q$ and that the axial thrust in the beam H can be regarded as constant by the assumption of small curvature, the equation of equilibrium is obtained:

$$EI \, \frac{d^4(y - y_0)}{dx^4} + H \, \frac{d^2 y}{dx^2} - H_0 \, \frac{d^2 y_0}{dx^2} = -q \tag{6}$$

To find the thrust H, it is noted that the shortening of the center line of the beam is

$$\Delta L \doteq \frac{1}{2} \int_0^L \left[\left(\frac{dy_0}{dx}\right)^2 - \left(\frac{dy}{dx}\right)^2 \right] dx - \Delta \tag{7}$$

where small quantities of higher orders are neglected. It is assumed that the end support spring is rather strong, so that Δ is very small compared with L. (Otherwise the problem becomes one of a simple bending, with no possible difficulty.) Hence

$$H = H_0 + \frac{EA(\Delta L)}{L}$$

$$= H_0 + \frac{EA}{2L} \int_0^L \left[\left(\frac{dy_0}{dx}\right)^2 - \left(\frac{dy}{dx}\right)^2 \right] dx - \frac{EA}{L} \Delta \tag{8}$$

On the other hand, the deflection Δ is connected with the spring constant α by equation (1). Eliminating Δ between equations (1) and (8), substituting equations (2) and (3) for y and y_o into the result, and integrating, there is obtained

$$H = H_o + \beta \frac{\pi^2 EA}{4} \sum_m m^2 \left(a_m^2 - b_m^2 \right) \tag{9}$$

where

$$\beta = \frac{\alpha}{\alpha + \dfrac{EA}{L}} \tag{10}$$

Substituting equations (2) and (3) again into equation (6) and using equation (9), there is obtained now the equation of equilibrium expressed in terms of the Fourier coefficients:

$$-q = \frac{\pi^4 EI}{L^3} \sum_m m^4 (b_m - a_m) \sin \frac{m\pi x}{L} + \frac{H_o \pi^2}{L} \sum_m m^2 (a_m - b_m) \sin \frac{m\pi x}{L} -$$

$$\beta \frac{\pi^4 EA}{4L} \left[\sum_m m^2 \left(a_m^2 - b_m^2 \right) \right] \sum_m m^2 b_m \sin \frac{m\pi x}{L} \tag{11}$$

The boundary conditions are already satisfied.

Expand $q = q_o f(x)$ into a Fourier series:

$$q = q_o f(x) = q_o \sum_m k_m \sin \frac{m\pi x}{L} \tag{12}$$

where

$$k_m = \frac{2}{L} \int_0^L f(x) \sin \frac{m\pi x}{L} \, dx$$

On equating the coefficients of the corresponding terms in the right-hand sides of equations (11) and (12), there is obtained a set of an infinite number of simultaneous equations:

$$\beta \; \frac{\pi^4 EA}{4L} \left[\sum_{n=1}^{\infty} n^2 \left(b_n^2 - a_n^2 \right) \right] m^2 b_m + \left(\frac{\pi^4 EI m^4}{L^3} - \frac{H_0 \pi^2 m^2}{L} \right) (b_m - a_m) = -k_m$$

$$(m = 1, 2, 3, \ldots) \quad (13)$$

To simplify the expressions, introduce the following notations:

$$\left. \begin{array}{cc} \lambda_m = \dfrac{a_m L}{2} \sqrt{\dfrac{A}{I}} & B_m = \dfrac{b_m L}{2} \sqrt{\dfrac{A}{I}} \\[4mm] R = \dfrac{q_0 L^4}{2\pi^4 EI} \sqrt{\dfrac{A}{I}} & S = \dfrac{H_0 L^2}{\pi^2 EI} \end{array} \right\} \quad (14)$$

Then equations (13) become

$$B_m \left(\beta \sum_{n=1}^{\infty} n^2 B_n^2 - \beta \sum_{n=1}^{\infty} n^2 \lambda_n^2 + m^2 - S \right) = - \frac{R}{m^2} k_m + \lambda_m (m^2 - S)$$

$$(m = 1, 2, 3, \ldots) \quad (15)$$

Here λ_m and B_m represent the rise of the arch, being half the ratio of the amplitude of the mth harmonic in the initial and the deflected curve to the radius of gyration of the beam cross section; R is a dimensionless quantity specifying the lateral loading; and S is the ratio of the initial axial compression to the Euler column buckling load of the beam. Now $f(x)$, λ_n, and S are known in the problem; it remains to find the relation between R and B_m, from which the correspondence between the load and deflection can be traced and the stability of the beam determined.

Sometimes the Fourier series of the moment curve converges much faster than that of the loading itself. In such cases it is advantageous to use equations (4) and (5) directly instead of equation (6). Let the static bending moment of the lateral loading alone be written as M_0:

$$M_O = q_O L^2 F(x) \tag{16}$$

where q_O is a characteristic lateral pressure with the physical dimensions of force per unit length of the beam. Let $F(x)$ be expanded into a Fourier series, so that

$$M_O = q_O L^2 \sum_{m=1}^{\infty} K_m \sin \frac{m\pi x}{L} \tag{17}$$

where

$$K_m = \frac{2}{L} \int_0^L F(\xi) \sin \frac{m\pi \xi}{L} d\xi$$

Following the same reasoning as before, one arrives at the equations:

$$B_m \left(\beta \sum_{n=1}^{\infty} n^2 B_n^2 - \beta \sum_{n=1}^{\infty} n^2 \lambda_n^2 + m^2 - S \right) = -\pi^2 K_m R + \lambda_m (m^2 - S)$$

$$(m = 1, 2, 3, \ldots) \tag{18}$$

Both equations (15) and (18) will be used later. They are a system of an infinite number of simultaneous equations for which a general treatment is not known. However, there are many important cases where the number of equations can be reduced into a finite number; then a complete discussion is possible. Several examples will be given below.

Equations (4) and (5) may be written as

$$\frac{d^2 y}{dx^2} + \frac{H}{EI} y = \frac{d^2 y_O}{dx^2} + \frac{M_O(x)}{EI} + \frac{H_O}{EI} y_O$$

$$= G(x) \tag{19}$$

where $G(x)$ is a known function. The general solution is

$$y = C_1 \cos \nu x + C_2 \sin \nu x + \frac{1}{\mu} \int_0^x G(t) \sin \nu(x - t)\, dt \qquad (20)$$

where

$$\nu = \sqrt{\frac{H}{EI}}$$

The constants C_1 and C_2 must be determined according to the boundary conditions at the ends $y = 0$ for $x = 0$ and L. The solution $y(x)$ can then be substituted into equation (8) and ν computed. This gives a relation between ν and the external load. Biezeno and Friedrichs based their calculations on this relationship. Marguerre, on the other hand, used the energy principle and the methods of Ritz and Galerkin to obtain approximate solutions. The method of the present paper, based on the Fourier analysis, is due to the work of Y. S. Huang.[3] Recently, the same method was used by Hoff and Bruce (reference 6).

It is clear from equation (20) that the deflection and the critical load are continuous functionals of $y_o(x)$ and $M_o(x)$. Hence infinitesimal changes in $y_o(x)$ and $M_o(x)$ would always cause an infinitesimal change in the critical load.

SINUSOIDAL ARCH UNDER SINUSOIDAL LOADING

Consider the simplest case of a low sinusoidal arch subjected to a sinusoidal load distribution:

$$\left.\begin{aligned} y_o &= a_1 L \sin \frac{\pi x}{L} \qquad (0 < a_1 \ll 1) \\[2ex] q &= q_o \sin \frac{\pi x}{L} \end{aligned}\right\} \qquad (21)$$

[3] Professor of Aeronautics, Central University, Nanking, China.

The general equations of equilibrium (15) then become, in this
particular case,

$$
B_1\left(\beta \sum_{n=1}^{\infty} n^2 B_n^2 - \beta\lambda_1^2 + 1 - S\right) = -R + \lambda_1(1 - S)
$$

$$
B_2\left(\beta \sum_{n=1}^{\infty} n^2 B_n^2 - \beta\lambda_1^2 + 4 - S\right) = 0
$$

. . . .   (22)

$$
B_m\left(\beta \sum_{n=1}^{\infty} n^2 B_n^2 - \beta\lambda_1^2 + m^2 - S\right) = 0
$$

. . . .

This set of equations must be solved for B_m. In order to get a
qualitative investigation into the nature of the solution, first consider
the simplest case of an arch rigidly hinged at both ends, so that $\alpha = \infty$
or $\beta = 1$, and with zero initial axial thrust $S = H_o = 0$. The more
general case will be considered later.

An obvious set of solutions of equations (22) is

$$
B_2 = B_3 = \ldots = 0
$$

$$
B_1^3 - B_1\left(\lambda_1^2 - 1\right) = \lambda_1 - R
$$ (23)

If the relation between B_1 and R is plotted, the curves in
figure 4 are obtained. Depending upon the values of λ_1, there are
several possibilities: (1) If $\lambda_1 \lesseqgtr 1$, the curves have monotonic slope;
consequently, they determine the load-deflection curve uniquely. There
is no question of instability. (2) If $\lambda_1 > 1$, then there are two real
extremes and, for values of R in between these extremes, every loading
may have three possible positions of equilibrium. Following, for example,
curve IV in figure 4, the deformation of the beam can be traced as follows:
When the lateral loading is gradually increased from the starting point a,
the deflection gradually increases according to curve IV (the rise of the

arch decreases). When the point M is reached, any further increase of loading will make the beam jump to the configuration corresponding to the point N and then follow the right-hand branch of the curve. In between M and N, any increase in deformation needs no addition of loading and therefore is unstable. Hence M is the critical point, with the critical condition given by

$$\left.\begin{array}{c} \dfrac{dR}{dB_1} = 0 \\[4mm] \dfrac{d^2R}{dB_1^2} < 0 \end{array}\right\} \tag{24}$$

From equations (23) and (24), the critical values of B_1 and R can be obtained:

$$\left.\begin{array}{c} \left(B_1\right)_{cr} = \sqrt{\dfrac{\lambda_1^2 - 1}{3}} \\[6mm] R_{cr} = \lambda_1 + \sqrt{\dfrac{4}{27}\left(\lambda_1^2 - 1\right)^3} \end{array}\right\} \tag{25}$$

If $\lambda_1 < 1$, R_{cr} is imaginary; hence no instability will occur. This checks with the former discussion based on the uniqueness of the load-deflection curve.

The above solution, equations (23), however, is not unique. Equations (22) can allow a solution with one B_n, in addition to B_1, to be different from zero.[4] In this case

$$\left.\begin{array}{c} B_1\left(B_1^2 + n^2B_n^2\right) - \left(\lambda_1^2 - 1\right)B_1 = \lambda_1 - R \\[4mm] B_1^2 + n^2B_n^2 = \lambda_1^2 - n^2 \end{array}\right\} \tag{26}$$

---

[4]These two cases exhaust the possibilities, as can be seen by writing down the rest of the set of equations (22), which gave the result that all other B's must vanish.

have the solution

$$B_1 = \frac{R - \lambda_1}{n^2 - 1}$$

$$n^2 B_n{}^2 = \lambda_1{}^2 - n^2 - \left(\frac{R - \lambda_1}{n^2 - 1}\right)^2$$
$$\left.\right\} \quad (27)$$

Equations (27) indicate that B_n can exist (with real value) only in a definite range of R. The deformation history of a beam subjected to gradually increasing lateral loading can now be traced as in figure 5: Along ab, $B_n = 0$, the curve is that of equations (23). Along bc, $B_n \neq 0$, the deflection curve becomes

$$y = b_1 L \sin \frac{\pi x}{L} + b_n L \sin \frac{n \pi x}{L} \qquad (28)$$

If the point b is real and lower than M, then it is the critical point where the beam will have a tendency to buckle. The point b is given by

$$B_1 = \sqrt{\lambda_1{}^2 - n^2}$$

$$B_n = 0$$
$$\left.\right\} \quad (29)$$

$$R = \lambda_1 - (n^2 - 1)\sqrt{\lambda_1{}^2 - n^2}$$

Equations (29) will yield the lowest critical value if the following conditions are satisfied:

(1) R, B_1, and B_n are real

(2) The R given by equations (29) is less than the R given by equations (25)

(3) The B_1 given by equations (29) must be greater than that given by equations (25); otherwise, the beam will buckle in the first mode, at point M

(4) The particular number n is so chosen that the corresponding R_{cr} is a minimum

Conditions (1), (2), and (3) are satisfied if and only if

$$\lambda_1^2 \geqq \frac{3}{2}\left(n^2 - \frac{1}{3}\right) \tag{30}$$

Condition (4) is satisfied only if n = 2. Hence the complete expression for the critical loading is obtained:

$$\left. \begin{aligned} R_{cr} &= \lambda_1 + \sqrt{\frac{4}{27}\left(\lambda_1^2 - 1\right)^3} \qquad &(1 \leqq \lambda_1 < \sqrt{5.5}) \\ \\ R_{cr} &= \lambda_1 + 3\sqrt{\lambda_1^2 - 4} \qquad &(\lambda_1 \geqq \sqrt{5.5}) \end{aligned} \right\} \tag{31}$$

The relation between the critical loading and the beam-rise ratio is illustrated in figure 6. The solid lines are the actual critical conditions. The dashed lines are either imaginary or not the lowest critical load.

It is interesting to note here that for $\lambda_1 < \sqrt{5.5} \approx 2.345$ the buckling mode of a low sinusoidal arch is symmetrical but for $\lambda_1 > \sqrt{5.5}$ the buckling mode imitates that of a high arch, for which the deformation is essentially inextensional. As illustrated in figure 7, the arch deflects (flattens) at first under the increasing lateral loading from the initial position I to the state II, when the second mode B_2 starts entering into the picture. The mode of the beam during buckling, when it jumps from the upper to the lower side, is a curve like III in figure 7.

EFFECT OF INITIAL AXIAL COMPRESSION

Still restricting this discussion to the simple case of a sinusoidal arch under a sinusoidal loading and with fixed hinged supports at both ends, let an initial compressive force H_0 act on the beam, so that

$$S = \frac{H_0 L^2}{\pi^2 EI}$$

is different from zero, S being the ratio of the initial axial compression to the Euler column buckling load of the beam. The equation of equilibrium is given by equations (22) with $\beta = 1$. The solution of this set of equations is again either

$$B_1 \neq 0, \quad B_2 = B_3 = \ldots = 0$$

or

$$B_1 \neq 0, \quad B_n \neq 0, \quad \text{all the other } B_m\text{'s vanish}$$

One is led to the following conclusions:

For $\sqrt{1 - S} < \lambda_1 \leqq \sqrt{5.5 - S}$,

$$R_{cr} = (1 - S)\lambda_1 + \sqrt{\frac{4}{27}\left(\lambda_1^2 + S - 1\right)^3}$$

and for $\lambda_1 > \sqrt{5.5 - S}$,

$$R_{cr} = (1 - S)\lambda_1 + 3\sqrt{\lambda_1^2 + S - 4}$$

(32)

The effect of the initial axial compression is included in this formula. As expected, the increase of the initial axial compression will decrease the critical load, as can be easily verified by the fact that

$$\frac{\partial R_{cr}}{\partial S} < 0 \tag{33}$$

for the full range of S, $0 \leqq S \leqq 1$ (S cannot exceed 1). Furthermore, the lower limit for instability is now

$$\lambda_1 = \sqrt{1 - S} \tag{34}$$

For λ_1 smaller than this value, the bar is stable; no buckling is possible. This lower limit decreases with increasing S until $S = 1$, when the beam will fail as a simple Euler column, R_{cr} becoming zero.

The values of the critical load R_{cr} as a function of λ_1, with values of S as parameters, are given in figure 6 and table I. A clearer presentation of the effect of S is a curve of the change in the critical load $\left(\Delta R_{cr}\right)_S$ against λ_1, where

$$\left(\Delta R_{cr}\right)_S = \left(R_{cr}\right)_{S=0} - \left(R_{cr}\right)_{S=S} \tag{35}$$

This is given in figure 8.

From equations (32), it is seen that when λ_1 is large, say, with magnitude of the order of 2.5 or larger, $\left(\Delta R_{cr}\right)_S$ is almost linearly proportional to S. As a crude approximation, one may take

$$\left(\Delta R_{cr}\right)_S = S \frac{\left(R_{cr}\right)_{S=0}}{4} \tag{36}$$

INITIAL SHAPE OF ARCH OTHER THAN SINUSOIDAL

In order to find the effect of the irregularities in the initial shape of the arch on the buckling load, some simple cases of low arches whose center lines are nonsinusoidal will be considered. By comparing such solutions with the previous one, the significance of such variations in form can be estimated. Let the initial shape of the center line of the arch be given by the equation:

$$y_0 = a_1 L \sin \frac{\pi x}{L} + a_m L \sin \frac{m \pi x}{L} \tag{37}$$

(A few examples are shown in fig. 9.) Assume again for simplicity that the lateral loading q is sinusoidal, given by equation (20), and that the ends of the arch are hinged and without initial thrust, so that $H_0 = S = 0$ and $\beta = 1$. The fundamental equations (15) become

$$B_1 \left(\sum_n n^2 B_n^2 - \lambda_1^2 - m^2 \lambda_m^2 + 1 \right) = -R + \lambda_1$$

$$B_m \left(\sum_n n^2 B_n^2 - \lambda_1^2 - m^2 \lambda_m^2 + m^2 \right) = m^2 \lambda_m \qquad\qquad\qquad (38)$$

$$B_k \left(\sum_n n^2 B_n^2 - \lambda_1^2 - m^2 \lambda_m^2 + k^2 \right) = 0 \qquad (\text{for all } k \neq 1, m)$$

Again two possibilities exist: (1) A solution consists of $B_1 \neq 0$ and $B_m \neq 0$, but with all other B's vanishing; (2) a solution with one B_k, other than B_1 and B_m, different from zero. They must be discussed separately.

In the first case, B_m and R may be regarded as functions of B_1 and the second of equations (38) differentiated to determine dB_m/dB_1. From the sign of dB_m/dB_1 it can be observed that, when the load R is gradually increasing, the amplitude of B_m $\left(\text{i.e., } |B_m| \right)$ will increase irrespective of the initial sign of λ_m. Furthermore, by differentiating the first of equations (38) to obtain dR/dB_1, it can be observed that, in the prebuckling stage, the amplitude B_1 will decrease when the load R increases. Hence the critical condition is given by

$$\frac{dR}{dB_1} = 0 \qquad\qquad\qquad (39)$$

Carrying out the differentiation and reducing, the equation governing B_m at the critical condition is obtained:

$$B_m^4 + c B_m + d = 0 \qquad\qquad\qquad (40)$$

where

$$c = - \frac{2\lambda_1^2 + 2m^2 \lambda_m^2 - 3m^2 + 1}{2(m^2 - 1)} \lambda_m$$

$$d = - \frac{3m^2 \lambda_m^2}{2(m^2 - 1)}$$

Equation (40) can have at most two real roots. If the two real roots are different, then the one nearer to λ_m is the true critical value provided that the corresponding $(B_1)_{cr}$ and R_{cr} are also real. If equation (40) has no real root, then there is no critical load and the beam is stable.

With the critical value of B_m so determined, the critical values of B_1 and R can be obtained from equations (38) as follows:

$$
\left.
\begin{aligned}
\left(B_1\right)_{cr}^2 &= \frac{m^2 \lambda_m}{(B_m)_{cr}} + \lambda_1^2 - m^2\left[(B_m)_{cr}^2 - \lambda_m^2 + 1\right] \\[3mm]
R_{cr} &= \lambda_1 + (m^2 - 1)\left(B_1\right)_{cr} - m^2 \frac{\lambda_m}{(B_m)_{cr}}\left(B_1\right)_{cr}
\end{aligned}
\right\}
\tag{41}
$$

It is interesting to note here that the critical load is independent of the sign of λ_m. This is so because a change in sign of λ_m changes the sign of the roots $(B_m)_{cr}$ of equation (40). But since $(B_m)_{cr}/\lambda_m$ does not change sign, $\left(B_1\right)_{cr}$ from the first of equations (41) is not affected by the change in sign of λ_m. Hence the conclusion follows from the second of equations (41). This is rather unexpected. It shows that under sinusoidal loading the two apparently different curved beams in figures 9(b) and 9(c) have exactly the same critical load.

Equation (40) can be solved graphically or numerically. The results of such calculations for the cases $m = 2$ and 3 are given in figures 10(a) and 10(b). The magnification of the amplitude of the higher harmonic, initially at λ_m, into $(B_m)_{cr}$ at the critical point, is clearly seen from figure 10. The reduction of the critical load due to the presence of λ_m will be discussed later when the second possible solution is obtained. The parameter used in the curves of figure 10 is not λ_m but the deviation ratio:

$$
\delta = \frac{\lambda_m}{\lambda_1} = \frac{a_m}{a_1}
\tag{42}
$$

This ratio indicates the deviation from a sinusoidal form better than the parameter λ_m itself.

It remains to discuss the second possible solution which includes one nonvanishing B_k ($k \neq 1$, m). In this case the solution of equations (38) is

$$B_1 = \frac{R - \lambda_1}{k^2 - 1}$$

$$B_m = \frac{-m^2\lambda_m}{k^2 - m^2}$$

$$k^2B_k^2 = \lambda_1^2 + m^2\lambda_m^2 - k^2 - \frac{m^6\lambda_m^2}{\left(k^2 - m^2\right)^2} - \frac{\left(R - \lambda_1\right)^2}{\left(k^2 - 1\right)^2}$$

(43)

The relation between B_k and R is again an ellipse of a similar nature to that for a sinusoidal arch under sinusoidal loading. The instant when B_k will appear is the critical point. Hence the condition $B_k = 0$ leads to

$$R_{cr} = \lambda_1 + \left(k^2 - 1\right)\sqrt{\lambda_1^2 - k^2 + m^2\lambda_m^2\left[1 - \frac{m^4}{\left(k^2 - m^2\right)^2}\right]}$$

(44)

This will lead to a fundamental critical value if the four conditions enumerated under equations (29) are satisfied. Whether equations (41) or equation (44) gives the critical load depends on the initial shape of the beam.

If m = 2, equation (44) always gives a higher R_{cr} than equations (41). Hence the critical load is determined by equations (41). No B_3, B_4, and so forth can appear during buckling.

If $m \geq 3$, equation (44) with k = 2 gives the lowest R_{cr} provided that λ_1 is greater than a certain constant, say $\left(\lambda_1\right)_0$. For λ_1 less than $\left(\lambda_1\right)_0$, equations (41) give the lowest R_{cr}. The point $\left(\lambda_1\right)_0$ is the point of tangency of the curves of R_{cr} against λ_1 computed according to equations (41) and (44), respectively.

Again it is evident from equation (44) that the critical load is independent of the sign of λ_m.

The combined results of equations (41) and (44) are shown in figure 11, and the numerical results are given in tables II and III. In table II, $(B_m)_{cr}$ and R_{cr} computed according to equations (40) and (41) are listed. Comparing tables II and III, it is seen that in certain ranges of λ_1, equations (41) give the lower R_{cr}, while in another range equation (44) gives the lower R_{cr}. Furthermore, at smaller values of λ_1, even if $\lambda_1 > 1$, $(B_1)_{cr}$ and R_{cr} may become imaginary, as shown in table II. The physical meaning of this is that the process is then a continuous one. There is no sudden change of configurations. The beam, under bending, simply yields continuously to the increasing external load.

These examples illustrate the serious nature of the effect of the λ_m terms. When the loading is symmetrical, a very slight component of unsymmetry in the curved beam lowers the critical load considerably. For example, in case of a sinusoidal loading acting on a sinusoidal beam, an unsymmetrical second harmonic in the initial curve with an amplitude ratio of 1 percent in the initial form lowers the critical load by approximately 10 percent. The buckling mode is always unsymmetrical if the initial shape of the arch contains unsymmetrical modes.

On the other hand, for a symmetric loading, the effect of higher harmonics that are symmetrical is much less pronounced. A similar effect should be expected when the beam is sinusoidal but the lateral loading deviates from a sinusoidal distribution.

An important special arch form is a circular arc with a radius ρ_0. Within the present approximation, there may be written

$$y_0 = \frac{1}{2\rho_0} x(L - x) = \frac{4L^2}{\pi^3 \rho_0} \sum_{n=1,3,5,\ldots} \frac{1}{n^3} \sin \frac{n\pi x}{L} \qquad (45)$$

This corresponds to an arch rise of $L^2/8\rho_0$ at the center. The coefficients λ_m form a rapidly decreasing sequence. In fact,

$$a_1 = \frac{4L^2}{\pi^3 \rho_0} \qquad\qquad a_{2n} = 0$$

$$a_2 = 0 \qquad\qquad a_{2n+1} = \frac{1}{(2n + 1)^3} a_1$$

$$a_3 = \frac{1}{27} a_1$$

The effect of the higher harmonics is negligible. If a_5, a_7, and so forth are neglected, then the R_{cr} (sinusoidal loading) of a circular arch can be found from figure 11(b) or table III (m = 3) by taking

$$\delta \doteq \frac{\lambda_3}{\lambda_1} = \frac{1}{27}$$

The difference in R_{cr} is readily seen to be small.

To illustrate the fact that a_5, a_7, and so forth may be neglected without causing appreciable error, the case of the unsymmetrical buckling mode will be considered. Equations (43) should be modified, when k = 2, into

$$\sum_n n^2 B_n^2 = \sum_n n^2 \lambda_n^2 - 4$$

$$B_1 = \frac{R - \lambda_1}{3}$$

$$B_m = \frac{\lambda_1}{m(m^2 - 4)}$$

Now

$$\sum_{n=1,3,5,\ldots} n^2 \lambda_n^2 = \lambda_1 \sum_{n=1,3,5,\ldots} \frac{1}{n^4} = \left(1 + \epsilon_1\right)\lambda_1^2$$

$$\sum_{m=3,5,7,\ldots} m^2 B_m^2 = \sum_{m=3,5,7,\ldots} \frac{\lambda_1^2}{(m^2 - 4)^2} = \frac{\lambda_1^2}{25}\left(1 + \epsilon_2\right)$$

where

$$\epsilon_1 \doteq 0.01436$$

$$\epsilon_2 \doteq 0.07325$$

The critical load is given by the equation:

$$\left(\frac{R - \lambda_1}{3}\right)^2 + \left(1 + \epsilon_2\right)\frac{\lambda_1^2}{25} = \left(1 + \epsilon_1\right)\lambda_1^2 - 4$$

Neglecting the effect of λ_5, λ_7, and so forth on R_{cr} is to neglect the effect of ϵ_1 and ϵ_2 on the root R of this equation. It is clearly justifiable.

UNIFORMLY DISTRIBUTED PRESSURE

In this section the critical load of a sinusoidal arch under uniformly distributed pressure will be discussed. From the results of the preceding sections, it is expected that the deflected curve of the arch would not remain sinusoidal and that an unsymmetrical component would in general enter into the buckling mode. For simplicity, again consider a simple sinusoidal arch, with ends hinged and without initial end thrust, so that $\beta = 1$, $\lambda_2 = \lambda_3 = \ldots = 0$, and $S = 0$. The lateral pressure is denoted by q_o per unit length of the span. Hence the bending moment in the beam, due to the lateral forces alone, without counting the contribution of the axial thrust, is

$$M_o = \frac{1}{2} q_o x(L - x)$$

$$= q_o \frac{4L^2}{\pi^3} \sum_{n=1,3,5,\ldots} \frac{1}{n^3} \sin \frac{n\pi x}{L} \tag{46}$$

It is convenient here to use equations (18) because the Fourier series of M_o converges much faster than that of the lateral loading itself. From equations (18), there can be obtained

$$\left.
\begin{aligned}
B_m\left(\sum_n n^2 B_n^2 - \lambda_1^2 + m^2\right) &= -\frac{4}{\pi m^3} R + \delta_{1m}\lambda_1 \qquad (m = 1, 3, 5, \ldots) \\[2em]
B_m\left(\sum_n n^2 B_n^2 - \lambda_1^2 + m^2\right) &= 0 \qquad\qquad\qquad\qquad (m = 2, 4, 6, \ldots)
\end{aligned}
\right\} \tag{47}$$

where $\delta_{1m} = 1$ if $m = 1$; $\delta_{1m} = 0$ if $m \neq 1$.

It is evident that when the load is applied, $R \neq 0$, all the B's with an odd subscript would in general differ from zero. It is also clear from the second of equations (47) that only one of the B's with an even subscript can differ from zero, because $\sum n^2 B_n^2$ cannot be equal to two different values of $\lambda_1^2 - m^2$. As before, these two cases would be separately treated.

Consider first the simpler case in which one of the B's with an even subscript is different from zero. In this case the deflection curve of the beam is unsymmetrical. Let the nonvanishing B be B_{2k}, where k is an integer. From the second of equations (47), then

$$\sum_n n^2 B_n^2 = \lambda_1^2 - 4k^2 \tag{48}$$

Hence from the first of equations (47),

$$B_m = \frac{1}{m^2 - 4k^2}\left(-\frac{4}{\pi m^3} R + \delta_{1m}\lambda_1\right) \qquad (m = 1, 3, 5, \ldots) \tag{49}$$

Squaring B_m, multiplying by m^2, and summing, there is obtained

$$\sum_n n^2 B_n^2 = \frac{1}{\left(1 - 4k^2\right)^2}\left(\lambda_1 - \frac{4}{\pi} R\right)^2 +$$

$$\frac{16R^2}{\pi^2} \sum_{m=3,5,\ldots} \frac{1}{m^4\left(m^2 - 4k^2\right)^2} + 4k^2 B_{2k}^2 \tag{50}$$

Equating this to $\lambda_1^2 - 4k^2$ according to equation (48), an equation is obtained relating B_{2k} with R. This relation is an ellipse, as in the section "Sinusoidal Arch under Sinusoidal Loading." The critical condition is reached when

$$\frac{dR}{dB_{2k}} = 0$$

which implies that

$$B_{2k} = 0 \tag{51}$$

With condition (51), the critical load R_{cr} is given by the following equation derived from equations (48) and (50):

$$\frac{16}{\pi^2} R^2 \sum_{m=1,3,5,\ldots} \frac{1}{m^4(m^2 - 4k^2)^2} - \frac{8\lambda_1 R}{\pi(1 - 4k^2)^2} = \left[1 - \frac{1}{(1 - 4k^2)^2}\right]\lambda_1^2 - 4k^2 \tag{52}$$

The series in the coefficient of R^2 converges very fast. If all terms except the first one are neglected, the error is less than 1/2 percent. Hence equation (52) is essentially equivalent to

$$\left(\frac{4}{\pi} R - \lambda_1\right)^2 = \left(4k^2 - 1\right)^2\left(\lambda_1^2 - 4k^2\right) \tag{53}$$

Comparing this equation with equations (29) for the case of a sinusoidal arch under sinusoidal loading, it can be seen that they are almost identical except that R in equations (29) is replaced by $\frac{4}{\pi} R$ and n is written here as $2k$. One of the roots of equation (53) which would represent the critical load on the beam must satisfy the four conditions stated below equations (29). In a manner completely analogous to the treatment of sinusoidal loading under equations (29), one concludes that k must be equal to 1 and that the solution exists only when λ_1 is equal to or greater than $\sqrt{5.5}$. The critical load is then

$$R_{cr} \doteq \frac{\pi}{4}\left(\lambda_1 + 3\sqrt{\lambda_1^2 - 4}\right) = \frac{\pi}{4}\left(R_{cr}\right)_{\text{sine}} \qquad \left(\lambda_1 \geqq \sqrt{5.5}\right) \tag{54}$$

where $\left(R_{cr}\right)_{\text{sine}}$ means the critical R of a sinusoidally distributed lateral pressure.

If the full series in the coefficient of R^2 in equation (52) were taken, then, since $k = 1$, and

$$\sum_{m=3,5,7,\ldots} \frac{1}{m^4(m^2 - 4)^2} \doteq 4.977 \times 10^{-4}$$

equation (54) is modified by a factor of approximately (1 - 0.005), or

$$R_{cr} \doteq 0.995 \frac{\pi}{4} \left(R_{cr} \right)_{sine} \qquad \left(\lambda_1 \geqq \sqrt{5.5} \right) \quad (55)$$

Turning now to the other possible solution, that all the B's with an even subscript vanish, one sees by analogy to the case of a sinusoidal arch under sinusoidal loading that this mode of deformation would lead to a critical buckling load only if λ_1 is sufficiently small. Let

$$\sum_{n=1,3,5,\ldots} n^2 B_n^2 = C \tag{56}$$

Then equations (47) give

$$B_m = \frac{1}{C - \lambda_1^2 + m^2} \left(- \frac{4}{\pi m^3} R + \delta_{1m} \lambda_1 \right) \qquad (m = 1, 3, 5, \ldots) \quad (57)$$

From equations (57) compute $m^2 B_m^2$ and sum:

$$C = \sum_m m^2 B_m^2$$

$$= \frac{16}{\pi^2} R^2 \sum_{m=1,3,5,\ldots} \frac{1}{m^4 \left(C - \lambda_1^2 + m^2 \right)^2} -$$

$$\frac{8}{\pi} R \lambda_1 \frac{1}{C - \lambda_1^2 + 1} + \frac{\lambda_1^2}{C - \lambda_1^2 + 1} \tag{58}$$

This gives a relation between C and R but is rather useless because of its complexity. A more practical solution can be obtained by successive approximation. According to equations (57), for a given R, B_m decreases rapidly with increasing m. As a first approximation, then, neglect the effect of B_3, B_5, . . . and obtain from equations (47), m = 1, the equation of equilibrium:

$$B_1^3 - \left(\lambda_1^2 - 1 \right) B_1 = - \frac{4}{\pi} R + \lambda_1$$

which is again almost identical with equations (22) for the case of a sinusoidal arch under sinusoidal loading, except that R in equations (22) is now replaced by $\frac{4}{\pi} R$. Hence analogously,

$$
\left.\begin{aligned}
\left(B_1\right)_{cr} &\doteq \sqrt{\frac{\lambda_1^2 - 1}{3}} \\[2ex]
R_{cr} &\doteq \frac{\pi}{4}\left[\lambda_1 + \sqrt{\frac{4}{27}\left(\lambda_1^2 - 1\right)^3}\right] \\[2ex]
&= \frac{\pi}{4}\left(R_{cr}\right)_{sine} \qquad \left(1 \leqq \lambda_1 \leqq \sqrt{5.5}\right)
\end{aligned}\right\} \tag{59}
$$

For the second approximation, neglect the effect of B_5, B_7, and so forth, but consider B_3. Now equations (47) may be written as

$$
\left.\begin{aligned}
B_1\left(\sum_n n^2 B_n^2 - \lambda_1^2 + 9\right) &= -\frac{4}{\pi} R + \lambda_1 + 8B_1 \\[2ex]
B_3\left(\sum_n n^2 B_n^2 - \lambda_1^2 + 9\right) &= -\frac{4}{27\pi} R
\end{aligned}\right\} \tag{60}
$$

Hence at the buckling point,

$$
\left(\frac{B_3}{B_1}\right)_{cr} = \frac{-\dfrac{1}{27}\dfrac{4}{\pi} R_{cr}}{-\dfrac{4}{\pi} R_{cr} + \lambda_1 + 8\left(B_1\right)_{cr}} = \frac{\lambda_1 + \sqrt{\dfrac{4}{27}\left(\lambda_1^2 - 1\right)^3}}{\left(18\lambda_1^2 - 234\right)\left(B_1\right)_{cr}}
$$

Substituting into equations (60), which now become a relation combining B_1 and R, and using the criterion $dR/dB_1 = 0$ for buckling, there is obtained

$$\left(B_1\right)_{cr} = \sqrt{\frac{1}{3}\left(\lambda_1^2 - 1 - k\right)}$$

$$R_{cr} = \frac{\pi}{4}\left[\lambda_1 + \sqrt{\frac{4}{27}\left(\lambda_1^2 - 1 - k\right)^3}\right] \qquad \left(\lambda_1 < \sqrt{5.5}\right)$$

(61)

where

$$k = \frac{1}{36}\left[\frac{\lambda_1 + \sqrt{\frac{4}{27}\left(\lambda_1^2 - 1 - k\right)^3}}{\lambda_1^2 - 13}\right]^2$$

(62)

Since k is always positive, the critical load R_{cr} given by equations (61) is always smaller than the first approximation given by equations (59). But the difference is really very small because $k \ll 1$. Values of k are given as a function of λ_1 in table IV.

Since $\left(B_m\right)_{cr}$ decreases very fast with increasing m, the convergence of the successive approximation is very good. From a comparison of equations (62) and (59), there appears no need for further approximations.

It can be concluded that, with an error less than 1/2 percent, the critical value of R for a uniformly distributed loading is equal to $\pi/4$ times that of a sinusoidal loading.

Interpreting the result somewhat differently, compare the total load that an arch can carry when the load is distributed first uniformly and then sinusoidally. Let W be the total load. Then since

$$W_{unif} = q_o L$$

and

$$W_{sine} = \frac{2}{\pi} q_o L$$

and since R_{cr} is based on q_o,

$$\frac{\left(W_{cr}\right)_{sine}}{\left(W_{cr}\right)_{unif}} = \frac{\frac{2}{\pi}\left(R_{cr}\right)_{sine}}{\left(R_{cr}\right)_{unif}} = \frac{2/\pi}{\pi/4} = \frac{8}{\pi^2}$$

(63)

Expressed in words, if W is the total lateral load an arch can sustain without buckling when the load is distributed uniformly over the span, then the same arch can sustain only a total load of $\frac{8}{\pi^2} W$ if that load is distributed sinusoidally. Thus concentrating a load toward the center of the arch lowers the critical buckling load.

CENTRAL CONCENTRATED LOAD ON A SINUSOIDAL ARCH

The case of a concentrated load acting at the midpoint of the span can be analyzed in the same manner as for the case in the preceding section. Only a very brief explanation will be given below.

Assume again that the arch is initially sinusoidal, rigidly hinged at both ends and without initial end thrust, so that $\beta = 1$, $\lambda_2 = \lambda_3 = \ldots = 0$, and $S = 0$. The lateral load is written as

$$W = q_o L \qquad (64)$$

The bending moment due to the lateral forces alone is

$$M_o = \begin{cases} \frac{1}{2} Wx & \text{for } \left(0 \leqq x \leqq \frac{L}{2}\right) \\ \\ \frac{1}{2} W(L - x) & \text{for } \left(\frac{L}{2} \leqq x \leqq L\right) \end{cases} = 2 \frac{WL}{\pi^2} \sum_{m=1,3,5,\ldots} (-1)^{\frac{m-1}{2}} \frac{1}{m^2} \sin \frac{m\pi x}{L} \qquad (65)$$

The equations of equilibrium are

$$B_m\left(\sum_n n^2 B_n^2 - \lambda_1^2 + m^2\right) = -\sin \frac{m\pi}{2} \frac{2}{m^2} R + \delta_{1m}\lambda_1$$

$$(m = 1, 2, 3, \ldots) \qquad (66)$$

For the unsymmetric mode of buckling, if this mode is possible, the lowest R_{cr} occurs when $B_2 \neq 0$, which implies that

$$\sum_n n^2 B_n^2 = \lambda_1^2 - 4$$

and the critical load is given by the smallest positive root of the equation:

$$4R^2 \sum_{m=1,3,5,\ldots} \frac{1}{m^2(m^2-4)^2} - \frac{4\lambda_1}{9} R - \frac{8}{9}\lambda_1^2 + 4 = 0$$

Letting

$$\sum_{m=1,3,5,\ldots} \frac{1}{m^2(m^2-4)^2} = \frac{1+\epsilon}{9}$$

where ϵ is approximately 0.0409,

$$R_{cr} = \frac{1}{2(1+\epsilon)}\left[\lambda_1 + 3\sqrt{\lambda_1 - 4 + \left(\frac{8}{9}\lambda_1^2 - 4\right)\epsilon}\right] \tag{67}$$

or

$$R_{cr} \doteq \frac{1}{2}\left(R_{cr}\right)_{sine}$$

The numerical results of equation (67) which are used in the testing program are tabulated in table V and compared with $\frac{1}{2}\left(R_{cr}\right)_{sine}$ in figure 12. For the symmetrical mode of buckling, steps analogous to those in the preceding section lead to

$$R_{cr} = \frac{1}{2}\left[\lambda_1 + \sqrt{\frac{4}{27}\left(\lambda_1^2 - 1 - k'\right)^3}\right] \qquad \left(\lambda_1 < \sqrt{5.5}\right) \tag{68}$$

where

$$k' = 9k$$

k being the constant given by equation (62) and table IV.

Hence R_{cr} for a concentrated load is approximately equal to one-half of R_{cr} for a sinusoidally distributed load.

As in the preceding section compare the load carrying capacity of a low arch with respect to various distributions of the loading. Thus

$$
\left.
\begin{aligned}
\frac{\left(W_{cr}\right)_{conc}}{\left(W_{cr}\right)_{sine}} &\doteq \frac{1/2}{2/\pi} = \frac{\pi}{4} \\[3mm]
\frac{\left(W_{cr}\right)_{sine}}{\left(W_{cr}\right)_{unif}} &\doteq \frac{8}{\pi^2} \\[3mm]
\frac{\left(W_{cr}\right)_{conc}}{\left(W_{cr}\right)_{unif}} &\doteq \frac{8}{\pi^2} \times \frac{\pi}{4} = \frac{2}{\pi}
\end{aligned}
\right\}
\tag{69}
$$

These ratios are within 2 percent of the corresponding ratios of the total loads causing equal center deflections of a simply supported beam under the three load distributions. This indicates that, for any symmetrical load distribution, the buckling load W_{cr} is proportional to the total load (of the specified distribution) which causes unit center deflection of a straight simply supported beam.[5]

CENTRAL CONCENTRATED LOAD ON A NONSINUSOIDAL ARCH

Because the experiments to be described were carried out on a series of approximately sinusoidal arches with a central concentrated load, a more complete investigation of this case will be made. First the case $\lambda_1 \neq 0$ and $\lambda_3 \neq 0$ will be studied and the difference in the influence of λ_3 on R_{cr} for sinusoidal load and R_{cr} for a central load will be shown. Then the case in which $\lambda_1 \neq 0$, $\lambda_2 \neq 0$, and $\lambda_3 \neq 0$ will be investigated. The results of the second case are more complicated and are used principally to show when the simple superposition of the effects of λ_2 and λ_3 is not possible.

---

[5]This result was previously shown by Timoshenko (reference 1) for the case of symmetrical buckling mode.

For a pin-ended arch without initial thrust ($\beta = 1$, $S = 0$), the equation of equilibrium for a concentrated center load is

$$B_m \left[\sum_n n^2 \left(\lambda_n^2 - B_n^2 \right) - m^2 \right] = \frac{2R}{m^2} \sin \frac{m\pi}{2} - m^2 \lambda_m$$

$$(m = 1, 2, 3, \ldots) \quad (70)$$

If only $\lambda_1 \neq 0$ and $\lambda_3 \neq 0$, equations (70) become

$$
\left.
\begin{aligned}
B_1 \left(\lambda_1^2 + 9\lambda_3^2 - \sum_n n^2 B_n^2 - 1 \right) &= 2R - \lambda_1 \\[2em]
B_2 \left(\lambda_1^2 + 9\lambda_3^2 - \sum_n n^2 B_n^2 - 4 \right) &= 0 \\[2em]
B_3 \left(\lambda_1^2 + 9\lambda_3^2 - \sum_n n^2 B_n^2 - 9 \right) &= -\frac{2}{9} R - 9\lambda_3
\end{aligned}
\right\}
\quad (71)
$$

For the case of buckling in the unsymmetric second mode one can solve for $\sum_n n^2 B_n^2$ from the second of equations (71). Substituting this into the other two of equations (71), solving the resulting equations for B_1 and B_3, and again forming the sum $\sum_n n^2 B_n^2$ an equation is obtained connecting R, λ_1, λ_3, and B_2. At the critical condition B_2 vanishes. Thus one arrives at an equation governing the critical load:

$$4R^2 \sum_{n=1,3,5,\ldots} \frac{1}{n^2 (n^2 - 4)^2} + R \left(-\frac{4}{9} \lambda_1 + \frac{36}{25} \lambda_3 \right) - \frac{8}{9} \lambda_1^2 + \frac{504}{25} \lambda_3^2 + 4 = 0$$

Letting

$$\sum_{n=1,3,5,\ldots} \frac{1}{n^2(n^2 - 4)^2} = \frac{k}{9}$$

$$k \doteq 1.0409$$

there is obtained

$$R_{cr} = \frac{1}{2k}\left[\lambda_1 - \frac{81}{25}\lambda_3 + \sqrt{\left(\lambda_1 - \frac{81}{25}\lambda_3\right)^2 + 4k\left(2\lambda_1^2 - \frac{1134}{25}\lambda_3^2 - 9\right)}\right] \qquad (72)$$

It is interesting to note that in contrast with the sinusoidal load case, the sign of λ_3 is important, and $\left(R_{cr}\right)_{conc}$ no longer approaches $\frac{1}{2}\left(R_{cr}\right)_{sine}$ unless $\frac{81}{25}\lambda_3 \ll \lambda_1$. In fact, the effect of λ_3 on the ratio $\left(R_{cr}\right)_{conc}\big/\left(R_{cr}\right)_{sine}$ can be appreciable.

The $\frac{81}{25}\lambda_3$ terms in equation (72) arise from the cross product in the squaring of the right-hand side of the last equation of equations (71) to obtain B_3^2. If the case is considered in which only λ_1 and λ_2 are different from zero, there is no corresponding cross product and therefore it can be expected that λ_2 will have the same proportional effect on R_{cr} for a centrally loaded arch as for a sinusoidally loaded arch. Physically this difference in the effect of λ_2 and λ_3 seems reasonable since the central load occurs at the maximum amplitude of the λ_3 wave, but at a node of the λ_2 wave.

For the case in which λ_1, λ_2, and λ_3 differ from zero it is known from the section "Initial Shape of Arch Other Than Sinusoidal" that buckling always occurs in the second mode and that the influence of the higher modes is small. Therefore all B_m's with $m > 3$ will be neglected. Letting $\beta = 1$ and $S = 0$, the equations of equilibrium are

$$B_1\left(\sum_1^3 n^2\lambda_n^2 - B_1^2 - 4B_2^2 - 9B_3^2 - 1\right) = 2R - \lambda_1 \qquad (73a)$$

$$B_2\left(\sum_1^3 n^2\lambda_n^2 - B_1^2 - 4B_2^2 - 9B_3^2 - 4\right) = -4\lambda_2 \qquad (73b)$$

$$B_3\left(\sum_1^3 n^2\lambda_n^2 - B_1^2 - 4B_2^2 - 9B_3^2 - 9\right) = -\frac{2}{9}R - 9\lambda_3 \qquad (73c)$$

These equations are to be solved for the critical values of B_1, B_2, B_3, and R under the critical condition $\partial R/\partial B_1 = 0$. The solution can be effected in the following steps:

(1) Eliminate R between equations (73a) and (73c) and use equation (73b) to obtain an equation connecting B_1 and B_2:

$$\left[\left(3 - 4\frac{\lambda_2}{B_2}\right)^2 + 9\left(5 + 4\frac{\lambda_2}{B_2}\right)^2\right]B_1^2 + 2\left(3 - 4\frac{\lambda_2}{B_2}\right)\left(\lambda_1 + 81\lambda_3\right)B_1 -$$

$$9\left(5 + 4\frac{\lambda_2}{B_2}\right)^2\left(\frac{4\lambda_2}{B_2} - 4B_2^2 + \sum n^2\lambda_n^2 - 4\right) + \left(\lambda_1 + 81\lambda_3\right)^2 = 0 \qquad (74)$$

(2) Differentiate equations (73a) and (73b) with respect to B_1 and use the critical condition $\partial R/\partial B_1 = 0$ and equation (73b) to obtain $\partial B_2/\partial B_1$ and $\partial B_3/\partial B_1$ at the critical point. The results are expressed in terms of B_1, B_2, and B_3.

(3) These expressions for $\left(\partial B_2/\partial B_1\right)_{cr}$ and $\left(\partial B_3/\partial B_1\right)_{cr}$ are substituted into equation (73a) after differentiating it with respect to B_1. Using the critical condition $\partial R/\partial B_1 = 0$ and eliminating B_3 through equation (73b), an equation for $\left(B_1\right)_{cr}$ in terms of $\left(B_2\right)_{cr}$ is obtained:

$$\left(B_1\right)_{cr}^2 = \frac{1}{16}\left[3 - 4\,\frac{\lambda_2}{\left(B_2\right)_{cr}}\right]\left[12\,\frac{\lambda_2}{\left(B_2\right)_{cr}} + \frac{10}{\lambda_2}\left(B_2\right)_{cr}^2 - 3 + 2\sum_n n^2\lambda_n^2\right] \quad (75)$$

By plotting equations (74) and (75) a compatible solution can be found. This solution will not hold for $\lambda_2 = 0$, but it is valid for $\lambda_3 = 0$, although no simplification will result. The results for a series of arches with $\lambda_2/\lambda_1 = 0.005$ and $\lambda_3/\lambda_1 = 0.04$, which are representative of the test specimens to be described in the experimental section, are tabulated in table VI and plotted in figure 12. Comparing this with figure 11 it is seen that the combined influence of λ_2 and λ_3 is stronger than the sum of their separate influences for lower values of λ_1; but for higher values of $\lambda_1\left(\lambda_1^2 > 5.5\right)$ the principle of superposition can be used. This is not unexpected since for low values of λ_1 the presence of λ_2 causes the mode of buckling to change from symmetrical to unsymmetrical and thus changes the influence of λ_3 on R_{cr}.

In figure 13 the process of loading is pictured for two examples in the above sequence of arches, one below the dividing value of $\lambda_1 = \sqrt{5.5}$ and one above. The changes in amplitudes of the three modes $\lambda_1 - B_1$, $B_2 - \lambda_2$, and $B_3 - \lambda_3$ are plotted as functions of the load R for $\lambda_1 = 2$ and $\lambda_1 = 4$. It is to be noted that, for the lower value of λ_1, B_2 does not increase rapidly until just before buckling occurs, while, for $\lambda_1 = 4$, B_2 starts increasing rapidly at a point appreciably before the buckling point. For both cases B_3 increases at an almost constant rate until just at the point of buckling.

ELASTIC SUPPORTS AT ENDS

So far the ends of the arch have been considered as rigidly hinged. Since ideal rigid hinges cannot be realized in the testing machine, it is expected that some deviation in the experimental buckling load from the theoretical value may exist owing to the yielding of the supports. In order to obtain some quantitative measure of the effect of support displacement, an example of an arch with elastic supports will be considered.

Assume that the supports are perfectly elastic. Let α be the spring constant of the support so that a displacement Δ would produce a thrust of magnitude $\alpha\Delta$. Without loss of generality it can be assumed that one end is rigidly hinged, and the other is elastically supported, as shown in figure 3. The effect of the support rigidity on the

equilibrium is expressed by the parameter β, defined by equation (10). The equations of equilibrium are either equations (15) or (18).

As an example, consider a sinusoidal arch loaded laterally by a sinusoidally distributed load of intensity q per unit length:

$$y_0 = a_1 L \sin \frac{\pi x}{L}$$

$$q = q_0 \sin \frac{\pi x}{L}$$

The equation of equilibrium is given by equations (22). The solution obtainable in the same manner as in the section "Sinusoidal Arch under Sinusoidal Loading" is

$$\left.\begin{array}{ll} R_{cr} = (1 - S)\lambda_1 + \sqrt{\dfrac{4}{27}\dfrac{\left(\beta\lambda_1{}^2 - 1 + S\right)^3}{\beta}} & \left(\dfrac{1}{\sqrt{\beta}} < \lambda_1 \leqq (\lambda_1)_0\right) \\[4ex] R_{cr} = (1 - S)\lambda_1 + 3\sqrt{\dfrac{\beta\lambda_1{}^2 - 4 + S}{\beta}} & \left(\lambda_1 > (\lambda_1)_0\right) \end{array}\right\} \quad (76)$$

where $(\lambda_1)_0$ is the smallest positive real root of the equation:

$$\left(\beta\lambda_1{}^2 - 4 + S\right) = \frac{4}{243}\left(\beta\lambda_1{}^2 - 1 + S\right)^3 \tag{77}$$

The effect of the nonrigidity of the support ($\beta < 1$) is shown in figure 14 and table VII. The values of $(\lambda_1)_0$ as a function of β are also given in that figure and table. The limiting case, $\alpha \longrightarrow \infty$ and $\beta \longrightarrow 1$, checks with the results of the sections "Sinusoidal Arch under Sinusoidal Loading" and "Effect of Initial Axial Compression."

If the support offers no resistance to the axial thrust, that is, it is perfectly flexible, then $\alpha = 0$ and $\beta = 0$. In this case there is no critical buckling load; the arch deflects continuously because the lower limit of λ_1, $1/\sqrt{\beta}$, below which no buckling can occur, now tends to infinity.

Similarly other loading conditions may be treated. For example, if β differs from 1, the ratios of R_{cr} for a uniformly distributed load, a sinusoidally distributed load, and a concentrated load at the center are again, respectively, $\pi/4$, 1, and 1/2.

LATERAL ELASTIC SUPPORTS

In application to certain wing design problems, it is desired to investigate the effect of lateral elastic supports on the buckling load of the arch. As an example, consider an arch having an elastic support at the center, as shown in figure 3. Let α' be the spring constant of the support. Then the change in thrust in the spring is

$$V = \alpha'\left[\Delta' - \left(\Delta'\right)_0\right] \tag{78}$$

where $\Delta' - \left(\Delta'\right)_0$ is the change in the deflection at the midspan. No generality is lost by assuming $\left(\Delta'\right)_0$ to be zero, if initial thrust in the spring is counted as a lateral force.

Now when the deflection curve of the arch is given by equations (2) and (3),

$$\Delta' - \left(\Delta'\right)_0 = \sum_{m=1,3,5,\ldots} (-1)^{\frac{m-1}{2}} (a_m - b_m)L \tag{79}$$

The moment contributed by V is then (cf. equation (65))

$$\left(M_0\right)_V = -\frac{2VL}{\pi^2} \sum_{m=1,3,5,\ldots} (-1)^{\frac{m-1}{2}} \frac{1}{m^2} \sin\frac{m\pi x}{L} \tag{80}$$

Combining equations (78), (79), and (80) and adding $\left(M_0\right)_V$ to the right-hand side of equation (4), there is obtained, after some reduction, the equations of equilibrium (equations (18) modified):

$$B_m\left(\beta \sum_n n^2 B_n^2 - \beta \sum_n n^2 \lambda_n^2 + m^2 - S\right) = -\pi^2 K_m R + \lambda_m\left(m^2 - S\right) +$$

$$\sin \frac{m\pi}{2} \frac{\mu}{m^2} \sum_{n=1,3,5,\ldots} (-1)^{\frac{n-1}{2}} \left(\lambda_n - B_n\right) \tag{81}$$

where K_m is given by equation (17) and

$$\mu = \frac{2L^3}{\pi^4 EI} \alpha' \tag{82}$$

Since a simply supported beam with a unit concentrated load at its center has a deflection of $\frac{1}{48} \frac{L^3}{EI} \approx \frac{2}{\pi^4} \frac{L^3}{EI}$ under the load, μ is approximately the ratio of α' to the spring constant of a simply supported beam having the linear dimensions of the arch.

Consider a sinusoidal arch subject to sinusoidal loading. For simplicity let the initial thrust be zero and let the end hinges be rigid. Then if $m \neq 1$,

$$\beta = 1$$

$$S = 0$$

$$\lambda_m = 0$$

$$K_1 = \frac{1}{\pi^2}$$

$$K_m = 0$$

The governing equations are

$$B_m\left(\sum_n n^2 B_n^2 - \lambda_1^2 + m^2\right) = -\delta_{1m}R + \delta_{1m}\lambda_1 +$$

$$\begin{cases} (-1)^{\frac{m-1}{2}} \dfrac{1}{m^2}\, \mu\left[\lambda_1 - \displaystyle\sum_{n=1,3,\ldots} (-1)^{\frac{n-1}{2}} B_n\right] & \text{(if } m \text{ is odd)} \\[2em] 0 & \text{(if } m \text{ is even)} \end{cases} \tag{83}$$

Let

$$\left. \begin{aligned} Q &= \lambda_1 - \sum_{n=1,3,\ldots} (-1)^{\frac{n-1}{2}} B_n \\[1em] P &= \sum_{n=1,3,\ldots} n^2 B_n^2 \end{aligned} \right\} \tag{84}$$

then

$$B_1 = \frac{\lambda_1 - R + 2\mu Q}{P + 1 - \lambda_1^2}$$

$$B_m = (-1)^{\frac{m-1}{2}} \frac{2\mu Q}{m^2\left(P + m^2 - \lambda_1^2\right)} \qquad (m \text{ odd and } \geq 3)$$

With these values for B_m, there is obtained

$$Q = \lambda_1 + \frac{R - \lambda_1}{P + 1 - \lambda_1^2} - \sum_m \frac{2\mu Q}{m^2\left(P^2 + m^2 - \lambda_1^2\right)} \tag{85}$$

First calculate the critical load for unsymmetric buckling where $B_{2n} \neq 0$ for some n. Then according to equations (83),

$$P = \lambda_1{}^2 - 4n^2 \tag{86}$$

But P is also given by

$$P = \sum_m m^2 B_m{}^2$$

$$= 4\mu^2 Q^2 \sum_{m=1,3,\ldots} \frac{1}{m^2(m^2 - 4n^2)^2} + \frac{(\lambda_1 - R)(\lambda_1 - R + 4\mu Q)}{(1 - 4n^2)^2} + 4n^2 B_{2n}{}^2 \tag{87}$$

Neglect all except the $m = 1$ term of the series and substitute the value of P from equation (86):

$$\frac{(\lambda_1 - R + 2\mu Q)^2}{(1 - 4n^2)^2} = \lambda_1{}^2 - 4n^2 - 4n^2 B_{2n}{}^2 \tag{88}$$

The critical condition is again $B_{2n} = 0$. Solving equation (85) for Q and substituting together with $B_{2n} = 0$ into equation (88), one obtains

$$R_{cr} = \lambda_1 + (4n^2 - 1)\left[\sqrt{\lambda_1{}^2 - 4n^2} + 2\mu \frac{\lambda_1 - \sqrt{\lambda_1{}^2 - 4n^2}}{(4n^2 - 1)(1 + 2\mu\alpha) + 2\mu}\right]$$

where

$$\alpha = \sum_{m=1,3,\ldots} \frac{1}{m^2(m^2 - 4n^2)}$$

This expression is a minimum for $n = 1$, hence

$$\alpha \doteq -0.3087$$

$$R_{cr} = \left(R_{cr}\right)_{sine} + \frac{2\mu}{3 + 0.147\mu}\left[4\lambda_1 - \left(R_{cr}\right)_{sine}\right]$$

\hfill (89)

These values are given in table VIII and plotted in figure 15 for $\mu = 0$, 0.5, 1, 1.5, 2, and 3.

In this solution the effect of the higher modes ($m \geqq 3$) on the force exerted by the spring, which enters by the series $\sum\limits_{m} \dfrac{1}{m^2(m^2 - 4)}$, is included, but the effect of the higher modes in lowering the buckling load, which enters by the faster converging series $\sum\limits_{m} \dfrac{1}{m^2(m^2 - 4)^2}$, is neglected. In the analogous case of the arch with a concentrated central load this results in a maximum error of 3 percent for $\lambda_1 < 10$ and for this case it should be no more.

Consider next the case of symmetrical buckling which occurs for the smaller values of λ_1. As a first approximation neglect the effects of all the B_m's except B_1. Then from equations (83), there is obtained under the critical condition $\partial R/\partial B_1 = 0$ the critical load:

$$R_{cr} = \lambda_1(1 + 2\mu) + \sqrt{\frac{4}{27}}\left(\lambda_1{}^2 - 1 - 2\mu\right)^{3/2}$$

\hfill (90)

A procedure similar to that used in the section "Initial Shape of Arch Other Than Sinusoidal" can be applied to find further approximations. The results of such a calculation, with the effects of B_1 and B_3 included, are given in table VIII and are plotted in figure 15.

BUCKLING LOAD BASED ON KÁRMÁN AND TSIEN'S ENERGY CRITERION

It is well-known that the classical buckling criterion, on which the calculations of the preceding sections are based, leads to erroneous

results for cylindrical and spherical shells; while a fundamentally different criterion, first proposed by Kármán and Tsien, whose latest version is given in reference 7, gives much closer agreement with experiments. The criterion of Kármán and Tsien (henceforth referred to as energy criterion) is that the buckling load is reached when the total energy in a possible (buckled) equilibrium state is equal to the total energy in the unbuckled state. In other words, if the total potential energy is such that it is permissible for the structure to jump from the unbuckled state to a buckled state, then the structure will actually jump.

Both the classical and the energy criteria have been applied to curved beams and shells. In some cases the classical criterion gives closer agreement with experiments; in others, the energy criterion gives better results. The reason, as pointed out by Tsien, is that in some cases the energy "hump" between two equilibrium states (one buckled and one unbuckled) of the same energy level is large and in other cases it is small. If the hump is small, the ever present small disturbances will enable the structure to jump from the unbuckled state to the more stable buckled state. Otherwise, this jump will be hindered. The crucial decision of the proper criterion depends much on what one means by a "practical" experimental setup or a "practical" service condition of the structure.

The energy criterion has been applied to the low arch problem by Friedrichs (reference 5) who found a great reduction in R_{cr} based on the energy criterion from that based on the classical criterion. In order to decide which criterion actually applies to the buckling of low arches, the experimental setup to be described in the next section will be accepted as practical and the theoretical results will be compared with experiments.

In applying the energy criterion, one must distinguish a constant deflection loading (a rigid testing machine) from a constant force (dead-weight) load. In the former case the change in total energy in buckling is just equal to the change in the internal strain energy, while in the latter case it is equal to the change in the strain energy minus the force times the displacement. However, a laterally loaded arch cannot buckle if the point of loading is not allowed to jump; hence only the dead-weight loading case will be considered.

For dead-weight loading the total energy is

$$\phi = U - W \tag{91}$$

where U is the strain energy and W is the work done by the lateral loading. The energy ϕ can be expressed as a function of the

deflection δ. Then according to the energy criterion, buckling would occur under a dead weight F provided that

$$
\left.
\begin{array}{c}
\phi(\delta_1) = \phi(\delta_2) \\[2ex]
F(\delta_1) = F(\delta_2)
\end{array}
\right\}
\tag{92}
$$

where δ_1 and δ_2 are two deflection configurations. Now the strain energy U, under the assumptions of the section "General Analysis," is given by

$$
U = \frac{1}{2} EI \int_0^L \left(\frac{d^2y}{dx^2} - \frac{d^2y_0}{dx^2} \right)^2 dx + \frac{\left(H^2 - H_0{}^2\right)L}{2AE}
\tag{93}
$$

From equations (2), (3), and (9), equation (93) becomes

$$
U = K \sum_m m^4 \left\{ (\lambda_m - B_m)^2 \left[1 + \frac{1}{2}(\lambda_m + B_m)^2 \right] + S\left(\lambda_m{}^2 - B_m{}^2\right) \right\}
\tag{94}
$$

where

$$
K = \frac{\pi^4 EI}{AL^3}
$$

The work done by the external load in the buckling process is

$$
W = \int_0^L q(y_0 - y)\, dx
\tag{95}
$$

For a sinusoidally distributed loading,

$$
W = 2KR(\lambda_1 - B_1)
\tag{96}
$$

while for a concentrated load at the midspan

$$W = 4KR \sum_{m=1,3,5,\ldots} (-1)^{\frac{m-1}{2}} (\lambda_m - B_m) \tag{97}$$

The buckling load according to the energy criterion can then be obtained easily.

Sinusoidally Distributed Loading on a Sinusoidal Arch

It was shown in the section "Sinusoidal Arch under Sinusoidal Loading" that the only equilibrium position of a sinusoidal arch under sinusoidally distributed load is the one for which all the B_m's $(m = 2, 3, \ldots)$ vanish. Hence if $S = 0$ (zero initial thrust),

$$\left. \begin{array}{l} \dfrac{\phi}{K} = (\lambda_1 - B_1)^2 \left[1 + \dfrac{1}{2}(\lambda_1 + B_1)^2 \right] - 2R(\lambda_1 - B_1) \\[3mm] R = \lambda_1 + B_1(\lambda_1{}^2 - 1) - B_1{}^3 \end{array} \right\} \tag{98}$$

The buckling conditions that $\phi(B_1') = \phi(B_1'')$ and $R(B_1') = R(B_1'')$ are fulfilled when $R = \lambda_1$ at which

$$\frac{\phi}{K} = B_1{}^2 - \lambda_1{}^2 + \frac{1}{2}(\lambda_1{}^2 - B_1{}^2)^2 \tag{99}$$

and $\phi(B_1) = \phi(-B_1)$. A substitution of $R = \lambda_1$ into the second of equations (98) gives the arch rise at the critical condition:

$$(B_1)_{cr} = \sqrt{\lambda_1{}^2 - 1}$$

or

$$(B_1)_{cr} = 0$$

Hence

$$R_{cr} = \lambda_1 \tag{100}$$

Central Concentrated Load on a Sinusoidal Arch

Assuming no initial thrust (S = 0), from equations (94) and (97)

$$\frac{\phi}{K} = \left(\lambda_1 - B_1\right)^2 \left[1 + \frac{1}{2}\left(\lambda_1 + B_1\right)^2\right] - 4R\left(\lambda_1 - B_1\right) +$$

$$\sum_{m=3,5,\ldots} \left[m^4 B_m^2\left(1 + \frac{1}{2} B_m^2\right) + 4R(-1)^{\frac{m-1}{2}} B_m\right] \qquad (101)$$

From equations (66)

$$2R = \lambda_1 - B_1\left(\sum_m m^2 B_m^2 - \lambda_1^2 + 1\right) \qquad (102)$$

If all the B_m's except B_1 are neglected, the above equations become identical with those for the sinusoidal loading if R is replaced by 2R. Thus approximately, R_{cr} for the concentrated center load is one-half of that for the sinusoidal load. This is the same approximate ratio as for R_{cr} of the sinusoidal and the concentrated loadings based on the classical criterion.

The ratio of R_{cr} based on the energy criterion to that based on the classical criterion is plotted in figure 16 for sinusoidal loadings on a sinusoidal arch. This same ratio holds approximately for the central load on sinusoidal arches.

EXPERIMENTS

A series of pin-ended arches having rigid simple supports were loaded with a central concentrated load in the testing apparatus shown in figures 17 and 18. The ideal end conditions were approximated as closely as possible by supporting the arches on knife edges mounted in a heavy steel frame having a stiffness approximately 100 times that of the specimen. Allowing a 20-percent reduction in this stiffness due to the flexibility of the knife edges and fittings results in a value of β equal to 0.988. A reference to the section "Elastic Supports at Ends" and figure 14 shows that a maximum error of about 1 percent will result from considering the supports as perfectly rigid.

The knife-edge fittings were provided with sockets which alined the ends of the specimen with the knife edges. (See fig. 19.)

The most critical problem in setting up the specimens for testing was the spacing of the supports. A looseness or an initial compression results in a change in the initial arch shape and an appreciable error in the buckling load. In the tests the spacing adjustment was made by a wedge controlled by a screw which was rotated until the play between the specimen and the knife edges was just eliminated.

The specimens were cut from 24S-T3 and 75S-T6 sheets and milled to 1/2-inch width. The strips were then rolled to the desired curvature on a three-roll roller. To reduce the effect of roll eccentricity several passes were made at each setting of the rolls, the rolls being indexed to a new position at the start of each pass.

The curvature of each specimen was measured at 12 stations by a dial gage which could be read up to ten-thousandths of an inch, placed between knife edges 2 inches apart. These curvatures were numerically integrated to find the shape of the specimen for which a 12-term Fourier expansion (half-range sine series) was made. The first three coefficients are given in table IX. As a check on the accuracy of the method the central rise of the arch as predicted by the numerical integration was compared with the actual rise as measured with a vernier height gage. The difference was no more than 4 percent of the arch rise for each specimen measured. The central arch rise as predicted by the Fourier coefficients agreed with the numerical integration within 1 percent.

The Fourier coefficients λ_1, λ_2, and λ_3 were used in calculating the theoretical critical load. In such calculations use is made of the fact noted in the section "Central Concentrated Load on a Nonsinusoidal Arch" that, whereas for smaller λ_1 $\left(\text{say, } \lambda_1 < 2.4\right)$ the joint effect of λ_2 and λ_3 on R_{cr} is not equal to the sum of the effects of λ_2 and λ_3 separately, for larger λ_1 $\left(\text{say, } \lambda_1 > 2.4\right)$ the effects of λ_2 and λ_3 are superposable. Hence for $\lambda_1 < 2.4$ the more exact method of the aforementioned section was used, but for $\lambda_1 > 2.4$ the effects of λ_2 and λ_3 were calculated separately and added together algebraically. The effect of λ_3 is given by equation (72). That of λ_2, according to the previous argument, can be obtained, percentagewise, from figure 11(a) or table III.

Although no attempt was made to determine the arch shape during the loading process, visual observation showed that the test performance at least approximately agreed with the theoretical predictions. The gradual increase in the third mode with the load, resulting in a flattening of the arch and then a reversal of curvature for the higher values

of λ_1, was noted. For values of $\lambda_1 > 2.4$ the rapid increase in the unsymmetric second mode just before buckling was quite evident. The clearest indication of the onset of buckling, however, was obtained by noticing the vibration of the specimen as the individual weights were applied. Even a very careful application resulted in a slight vibration in the fundamental mode. When the load approached within a few pounds of the critical load there was a rapid decrease in the frequency of this vibration. Further load applications were made in extremely small increments.

The theoretical and experimental results are listed in table IX and plotted in figure 16. In figure 16, the ordinate is the ratio of R_{cr} determined by the test to that computed theoretically according to the classical criterion. In the same figure, the dashed line shows the ratio of R_{cr} given by the energy criterion to that given by the classical criterion. This curve is based on the simple sinusoidal arch $\left(\lambda_2 = \lambda_3 = 0\right)$. For arches used in the experiment λ_2 and λ_3 were so small that the variation of the ratio $\left(R_{cr}\right)_{energy}/\left(R_{cr}\right)_{class}$ does not vary much from the dashed curve of the figure.

It is seen that the test results agree quite well with results based on the classical criterion for higher values of λ_1 but drop appreciably below them for the lower values. All the test values, however, lie above the energy criterion curve. Although calculations for the series of arches representing the test specimens indicate that buckling would occur for $\lambda_1 \gtrsim 1.05$, no buckling was observed for $\lambda_1 \lesssim 1.38$.

A calculation of the stresses in the specimens at buckling was made to determine if yielding occurred. With $H_o = 0$ and $\beta = 1$ the axial compressive force is given by equation (9). Using the nondimensional notation it becomes

$$\sigma_c = \frac{H}{A}$$

$$= \frac{\pi^2 EI}{AL^2} \sum_m m^2\left(\lambda_m{}^2 - B_m{}^2\right) \tag{103}$$

For a sinusoidal arch with a sinusoidal load all the B_m's except B_1 are zero at the critical buckling load and $\left(B_1\right)_{cr}{}^2 = \frac{1}{3}\left(\lambda_1{}^2 - 1\right)$ for $1 \leqq \lambda_1{}^2 \leqq 5.5$ and $\left(B_1\right)_{cr}{}^2 = \lambda_1{}^2 - 4$ for $\lambda_1{}^2 \geqq 5.5$. Therefore

$$\frac{(\sigma_c)_{cr}}{\sigma_P} = \frac{H_{cr}}{P} = \begin{cases} \frac{1}{3}\left(1 + 2\lambda_1^2\right) & \text{(for } 1 \leq \lambda_1^2 \leq 5.5) \\ \\ 4 & \text{(for } \lambda_1^2 \geq 5.5) \end{cases} \tag{104}$$

where $P = \pi^2 EI/L^2$ is the Euler buckling load of the beam and $\sigma_P = P/A$. Thus it can be seen that the critical compressive force is just equal to the Euler load if $\lambda_1 = 1$. As λ_1 increases the critical force increases until it reaches the Euler load for buckling in the second mode. At this point the arch buckles unsymmetrically and the critical compressive stress remains constant for all higher values of λ_1. This performance is also typical of symmetrical arches with a central concentrated load, but for arches with a slight asymmetry, as is the case for the specimens tested, the value $H_{cr}/P = 4$ is approached only as λ_1 becomes large. The values of H_{cr}/P for a series of arches are given in table VI.

The maximum bending stress at any point x is given by

$$\sigma_b = \frac{1}{2} Et\left(\frac{d^2 y}{dx^2} - \frac{d^2 y_0}{dx^2}\right) \tag{105}$$

where t is the thickness of the specimen. In terms of the nondimensional Fourier coefficients this becomes

$$\sigma_b = \frac{\pi^2 Et}{L^2} \sqrt{\frac{I}{A}} \sum_m m^2 (\lambda_m - B_m) \sin \frac{m\pi x}{L} \tag{106}$$

The bending stresses at the midspan were calculated for the series of arches with $\lambda_2 = 0.005\lambda_1$ and $\lambda_3 = 0.040\lambda_1$ which are representative of the actual test specimens. The results are shown in table VI together with the total maximum stress for $t = 0.25$. The total stress for any other thickness is obtained by multiplying the last column of table VI by the factor $16t^2$.

All the specimens tested had maximum stresses well below the yield stress of the material at the buckling point. Yielding occurred in the post-buckling stage for all the specimens except those having the very lowest values of λ_1.

CONCLUSIONS

A Fourier analysis has been used to solve the problem of buckling of low arches under a lateral loading acting toward the center of curvature. The conclusions may be summarized as follows:

1. For a sinusoidal arch under a sinusoidal loading, the analysis gives a very simple exact solution for the nonlinear equation of equilibrium. The critical load can be expressed as a simple function of the beam dimension parameters. On the basis of the classical buckling criterion, it is shown that the buckling mode is symmetrical for arches having a nondimensional parameter λ_1 less than $\sqrt{5.5}$ and is unsymmetrical for λ_1 greater than $\sqrt{5.5}$. This dividing value is affected somewhat by the initial thrust in the arch and the elasticity of the support.

2. For arch shapes other than sinusoidal but under sinusoidal loading, it is shown that symmetrical deviations have only minor effects on the buckling load, while unsymmetrical modes of deviation cause serious reduction of the buckling load. The buckling mode is always unsymmetrical if the initial shape of the arch contains unsymmetrical modes. For sinusoidal loading the critical load is independent of the sign of $\lambda_m(m > 1)$; thus a pair of different arches can have the same critical load.

3. For a load distribution that deviates from sinusoidal, the unsymmetrical components again have serious effects. The critical load will be dependent upon the sign of $\lambda_m(m > 1)$. For symmetrical load distributions, the buckling loads are approximately proportional to the total loads (under the respective distributions) that are required to produce a unit deflection at the center of a straight simply supported beam without axial restraint.

4. Comparison with experiments shows that the classical criterion of buckling is applicable for larger values of λ_1, say, $\lambda_1 > 3$. But the classical criterion overestimates the buckling load for very flat arches. The experimental buckling load is always higher than that estimated according to the energy criterion of Kármán and Tsien but has a tendency to approach that criterion as λ_1 decreases. For $\lambda_1 \longrightarrow 1$ (with exact value depending on the initial thrust and support conditions), the arch deflects continuously and there is no buckling phenomenon.

California Institute of Technology
     Pasadena, Calif., January 24, 1952

REFERENCES

1. Timoshenko, S.: Theory of Elastic Stability. First ed., McGraw-Hill
     Book Co., Inc., 1936.

2. Biezeno, C. B.: Das Durchschlagen eines schwach gekrümmten Stabes.
     Z.a.M.M., Bd. 18, Heft 1, Feb. 1938, pp. 21-30.

3. Marguerre, K.: Die Durchschlagskraft eines schwach gekrümmten Balkens.
     Sitzungsber. Berliner math. Gesell., Bd. 37, June 1938, pp. 22-40.

4. Marguerre, Karl: Über die Anwendung der energetischen Methode auf
     Stabilitätsprobleme. Jahrb. 1938, DVL, pp. 252-262. (Available in
     translation as NACA TM 1138.)

5. Friedrichs, K. O.: Lectures on Non-Linear Elasticity. Mimeo. notes
     by S. Schaaf. New York Univ., 1945.

6. Hoff, N. J., and Bruce, V. G.: Dynamic Analysis of the Buckling of
     Laterally Loaded Flat Arches. PIBAL Rep. 191, Contract Nonr-267 00,
     Office of Naval Res. and Polytechnic Inst. of Brooklyn, Oct. 1951.

7. Tsien, Hsue-Shen: A Theory for the Buckling of Thin Shells. Jour.
     Aero. Sci., vol. 9, no. 10, Aug. 1942, pp. 373-384.

TABLE I

VALUES OF R_{cr} AS A FUNCTION OF INITIAL THRUST AND ARCH RISE

λ_1 / S	$(1 - S)^{1/2}$	1.0	1.2	1.4	1.6	1.8	2.0
0	1.000000	1.000000	1.312338	1.762039	2.349955	3.090387	4.000000
.1	.853815	.912172	1.232735	1.680056	2.263209	2.997755	3.900829
.25	.649519	.798113	1.120608	1.562302	2.137273	2.862332	3.755138
.50	.353553	.636083	.950784	1.379012	1.938017	2.645717	3.520288
1.00	0	.384900	.665108	1.056166	1.576551	2.244738	3.079201

λ_1 / S	2.2	$(5.5 - S)^{1/2}$	2.4	2.6	3	3.5	4
0	5.096309	6.019436	6.379947	7.583975	9.708204	12.116843	14.392306
.1	4.990180	5.765646	6.251454	7.413459	9.474954	11.818911	14.035515
.25	4.833707	5.392701	6.053234	7.154805	9.123864	11.371428	13.500000
.50	4.580028	4.792269	5.709987	6.716641	8.535621	10.624117	12.606599
1.00	4.069398	3.674235	4.983975	5.817216	7.348470	9.124145	10.816653
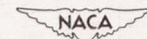
TABLE II

VALUES OF $(B_m)_{cr}$, $(B_1)_{cr}$, AND R_{cr} COMPUTED FROM EQUATIONS (40) AND (41)

(a) $m = 2$

λ_1	λ_2	$(B_2)_{cr}$	$(B_2)_{cr}/\lambda_2$	$(B_1)_{cr}$	R_{cr}	λ_2	$(B_2)_{cr}$	$(B_2)_{cr}/\lambda_2$	$(B_1)_{cr}$	R_{cr}
		$\lambda_2/\lambda_1 = 0.01$						$\lambda_2/\lambda_1 = 0.05$		
1.0	0.010	0.01334	1.334	Imag.[1]	Imag.	0.05	0.06655	1.331	Imag.	Imag.
1.2	.012	.01773	1.478	0.3828	1.312	.06	.08824	1.471	0.3785	1.306
1.4	.014	.02372	1.694	.5656	1.761	.07	.1170	1.672	.5635	1.742
1.6	.016	.03259	2.037	.7214	2.348	.08	.1569	1.961	.7257	2.297
1.8	.018	.04744	2.636	.8660	3.084	.09	.2121	2.357	.8886	2.958
2.0	.020	.07663	3.832	1.0110	3.978	.10	.2817	2.817	1.0690	3.689
2.2	.022	.1339	6.088	1.1947	4.999	.11	.3568	3.243	1.2699	4.443
2.4	.024	.1990	8.294	1.4443	6.036	.12	.4302	3.585	1.4808	5.190
2.6	.026	.2534	9.748	1.7077	7.022	.13	.5002	3.847	1.6931	5.919
3.0	.030	.3428	11.43	2.2099	8.856	.15	.6307	4.204	2.110	7.322
3.5	.035	.4386	12.53	2.7936	10.99	.175	.7840	4.480	2.609	8.997
4.0	.040	.5267	13.17	3.3467	13.02	.20	.9271	4.636	3.096	10.616
		$\lambda_2/\lambda_1 = 0.1$						$\lambda_2/\lambda_1 = 0.2$		
1.0	0.10	0.1325	1.325	Imag.	Imag.	0.20	0.2606	1.303	Imag.	Imag.
1.2	.12	.1742	1.451	0.3640	1.289	.24	.3349	1.396	0.2964	1.240
1.4	.14	.2264	1.617	.5540	1.692	.28	.4187	1.495	.4976	1.562
1.6	.16	.2910	1.818	.7235	2.179	.32	.5094	1.592	.6668	1.925
1.8	.18	.3662	2.035	.8940	2.724	.36	.6039	1.677	.8272	2.309
2.0	.20	.4473	2.237	1.0715	3.298	.40	.6998	1.749	.9838	2.702
2.2	.22	.5296	2.407	1.2542	3.879	.44	.7955	1.808	1.1381	3.096
2.4	.24	.6108	2.545	1.4388	4.455	.48	.8906	1.855	1.2902	3.489
2.6	.26	.6900	2.654	1.6226	5.022	.52	.9848	1.894	1.4403	3.879
3.0	.30	.8432	2.811	1.9848	6.130	.60	1.170	1.951	1.7354	4.648
3.5	.35	1.027	2.934	2.426	7.470	.70	1.398	1.997	2.096	5.590
4.0	.40	1.205	3.013	2.816	8.709	.80	1.622	2.028	2.450	6.518
		$\lambda_2/\lambda_1 = 0.3$						$\lambda_2/\lambda_1 = 0.4$		
1.0	0.30	0.3829	1.276	Imag.	Imag.	0.40	0.5002	1.250	Imag.	Imag.
1.2	.36	.4824	1.340	0.1111	1.202	.48	.6212	1.294	Imag.	Imag.
1.4	.42	.5879	1.400	.3746	1.453	.56	.7456	1.332	Imag.	Imag.
1.6	.48	.6968	1.452	.5429	1.733	.64	.8716	1.362	0.3177	1.612
1.8	.54	.8071	1.495	.6907	2.024	.72	.9980	1.386	.4637	1.853
2.0	.60	.9208	1.535	.8093	2.319	.80	1.124	1.405	.5916	2.091
2.2	.66	1.028	1.557	.9620	2.615	.88	1.250	1.421	.7082	2.331
2.4	.72	1.137	1.580	1.0911	2.911	.96	1.376	1.433	.8181	2.571
2.6	.78	1.246	1.598	1.2174	3.205	1.04	1.500	1.443	.9236	2.810
3.0	.90	1.463	1.625	1.4640	3.789	1.20	1.749	1.458	1.1242	3.288
3.5	1.05	1.730	1.648	1.7640	4.510	1.40	2.058	1.470	1.3688	3.881
4.0	1.20	1.996	1.663	2.0581	5.224	1.60	2.365	1.478	1.6048	4.471

[1]Imaginary.

NACA

TABLE II

VALUES OF $(B_m)_{cr}$, $(B_1)_{cr}$, AND R_{cr} COMPUTED FROM EQUATIONS (40) AND (41) - Concluded

(b)   m = 3

| λ_1	λ_3	$(B_3)_{cr}$	$(B_3)_{cr}/\lambda_3$	$(B_1)_{cr}$	R_{cr}	λ_3	$(B_3)_{cr}$	$(B_3)_{cr}/\lambda_3$	$(B_1)_{cr}$	R_{cr}
		$\lambda_3/\lambda_1 = 0.01$					$\lambda_3/\lambda_1 = 0.05$			
1.0	0.010	0.01125	1.125	Imag.	Imag.	0.05	0.05623	1.125	Imag.	Imag.
1.2	.012	.01402	1.168	0.3779	1.312	.06	.07001	1.167	0.3762	1.308
1.4	.014	.01712	1.223	.5647	1.762	.07	.08540	1.220	.5617	1.750
1.6	.016	.02069	1.293	.7342	2.364	.08	.1030	1.287	.7183	2.323
1.8	.018	.02490	1.383	.8622	3.088	.09	.1236	1.374	.8530	3.035
2.0	.020	.02998	1.499	1.0000	3.996	.10	.1473	1.473	1.0025	3.894
2.2	.022	.03642	1.655	1.1265	5.083	.11	.1758	1.598	1.1425	4.903
2.4	.024	.04460	1.858	1.2611	6.381	.12	.2098	1.748	1.2817	6.054
3.0	-----	-------	-----	------	-----	----	-------	-----	------	-----
4.0	-----	-------	-----	------	-----	----	-------	-----	------	-----
		$\lambda_3/\lambda_1 = 0.1$					$\lambda_3/\lambda_1 = 0.2$			
1.0	0.10	0.1112	1.122	0.1463	0.9969	0.20	0.2234	1.117	Imag.	Imag.
1.2	.12	.1395	1.162	.3693	1.295	.24	.2760	1.150	0.3172	1.255
1.4	.14	.1696	1.211	.5538	1.716	.28	.3321	1.186	.5110	1.610
1.6	.16	.2032	1.270	.7109	2.249	.32	.3919	1.225	.6694	2.036
1.8	.18	.2408	1.338	.8587	2.893	.36	.4549	1.264	.8163	2.516
2.0	.20	.2828	1.414	1.0025	3.649	.40	.5203	1.301	.9601	3.038
2.2	.22	.3292	1.496	1.1466	4.476	.44	.5877	1.336	1.101	3.589
2.4	.24	.3794	1.581	1.2950	5.386	.48	.6562	1.367	1.2416	4.159
2.6	.26	.4324	1.663	1.4486	6.348	.52	.7254	1.395	1.3821	4.740
3.0	----	------	-----	------	-----	.60	.8644	1.441	1.6620	5.913
4.0	----	------	-----	------	-----	.80	1.209	1.512	2.3557	8.821
		$\lambda_3/\lambda_1 = 0.3$					$\lambda_3/\lambda_1 = 0.4$			
1.0	0.30	0.3327	1.109	Imag.	Imag.	0.40	0.4402	1.101	Imag.	Imag.
1.2	.36	.4082	1.134	0.2086	1.213	.48	.5370	1.119	Imag.	Imag.
1.4	.42	.4867	1.159	.4133	1.501	.56	.6358	1.135	0.2668	1.420
1.6	.48	.5677	1.183	.5854	1.828	.64	.7360	1.150	.4428	1.677
1.8	.54	.6503	1.204	.7293	2.184	.72	.8371	1.163	.5833	1.951
2.0	.60	.7341	1.224	.8636	2.556	.80	.9385	1.173	.7100	2.233
2.2	.66	.8185	1.240	.9942	2.938	.88	1.040	1.182	.8283	2.520
2.4	.72	.9032	1.254	1.1216	3.326	.96	1.142	1.189	.9422	2.808
2.6	.78	.9881	1.267	1.2464	3.716	1.04	1.243	1.196	1.0525	3.097
3.0	.90	1.158	1.286	1.4932	4.496	1.20	1.446	1.205	1.2508	3.666
3.5	1.05	1.369	1.303	1.7944	5.465	1.40	1.699	1.213	1.5276	4.391
4.0	1.20	1.579	1.315	2.092	6.423	1.60	1.951	1.219	1.7818	5.101

NACA
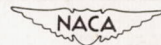
TABLE III

VALUES OF R_{cr} FOR A SINUSOIDALLY LOADED ARCH HAVING NONZERO λ_1 AND λ_m COMPUTED FROM EQUATION (44)

[Dashed lines indicate that there is no critical load]

(a) m = 3

λ_3/λ_1 \ λ_1	1.0	1.2	1.4	1.6	1.8	2.0	2.2	2.4	2.6	3.0	3.5	4.0
0.01	1.0000	1.3121	1.7615	2.3637	3.0881	3.9955	5.0877	6.3812	7.5720	9.6960	12.1039	14.3783
.05	------	1.3079	1.7499	2.3228	3.0349	3.8945	4.9029	6.0540	7.2662	9.3967	11.7881	14.0371
.1	------	1.2953	1.7161	2.2493	2.8926	3.6492	4.4765	5.3864	6.3485	8.3545	10.7127	12.8865
.2	------	1.2547	1.6105	2.0359	2.5164	3.0383	3.5892	4.1589	4.7396	5.9134	7.3769	8.8213
.3	------	1.2132	1.5011	1.8285	2.1840	2.5562	2.9384	3.3260	3.7159	4.4964	5.4650	6.4228
.4	------	------	1.4195	1.6772	1.9510	2.2332	2.5196	2.8081	3.0971	3.6657	4.3906	5.1012

(b) m = 2

λ_2/λ_1 \ λ_1	1.0	1.2	1.4	1.6	1.8	2.0	2.2	2.4	2.6	3.0	3.5	4.0
0.01	------	1.3121	1.7612	2.3476	3.0837	3.9775	4.9991	6.0364	7.0223	8.8561	10.9893	13.0235
.05	------	1.3060	1.7422	2.2970	2.9577	3.6889	4.4435	5.1904	5.9191	7.3218	8.9975	10.6163
.1	------	1.2887	1.6917	2.1790	2.7243	3.2982	3.8788	4.4548	5.0223	6.1296	7.4705	8.7094
.2	------	1.2397	1.5616	1.9248	2.3091	2.7019	3.0964	3.4892	3.8788	4.6475	5.5905	6.5179
.3	------	1.2017	1.4534	1.7328	2.0236	2.3185	2.6150	2.9106	3.2049	3.7888	4.5102	5.2240
.4	------	------	------	1.6120	1.8530	2.0910	2.3306	2.5705	2.8102	3.2878	3.8814	4.4714

TABLE IV

VALUES OF k FROM

EQUATION (62)

λ_1	k
1.0	0.1929×10^{-3}
1.2	.3578
1.4	.7075
1.6	1.408
1.8	2.767
2.0	5.486
2.2	10.83
2.4	21.70

TABLE V

VALUES OF R_{cr} FOR A SINUSOIDAL ARCH

WITH A CENTRAL CONCENTRATED LOAD

λ_1	R_{cr}
2.4	3.089
2.6	3.678
3.0	4.716
3.5	5.890
4.0	7.000
4.5	8.072
5.0	9.122
5.5	10.156
6.0	11.179
6.5	12.193
7.0	13.201
7.5	14.204
8.0	15.206
8.5	16.203
9.0	17.195

TABLE VI

CRITICAL CONDITIONS FOR CENTRALLY LOADED ARCHES WITH

$$\lambda_2 = 0.005\lambda_1 \quad \text{AND} \quad \lambda_3 = 0.040\lambda_1$$

λ_1	$(B_1)_{cr}$	$(B_2)_{cr}$	R_{cr}	$(B_3)_{cr}$	$\dfrac{(\sigma_c)_{cr}}{\sigma_p}$	$\dfrac{(\sigma_b)_{cr,max}}{\sigma_p}$	Max. critical stress (psi) [1]
1.2	0.3713	0.0088	0.651	0.075	1.28	3.85	8.4×10^3
1.5	.6310	.01351	.996	.108	1.84	4.50	10.4
2.0	.9895	.03263	1.878	.196	2.79	7.21	16.3
2.5	1.4003	.1157	3.048	.290	3.57	9.74	21.8
3.0	1.9770	.2175	4.193	.380	3.73	11.63	25.1
4.0	3.0494	.3605	6.236	.541	3.78	15.16	30.9
5.0	4.039	.4831	8.140	.693	3.79	18.7	36.8
6.0	4.990	.5991	9.986	.842	3.80	22.3	42.6
7.0	5.922	.7120	11.800	.990	3.80	25.9	48.5
8.0	6.841	.8231	13.596	1.136	3.81	29.5	54.5
9.0	7.752	.9332	15.380	1.282	3.81	33.1	60.3

[1]Highest outer fiber stress in arches representative of test speci-
mens $\left(E = 10.3 \times 10^6 \text{ psi}, \quad L = 18 \text{ in.}, \quad \text{and} \quad t = 0.25 \text{ in.}\right)$.   NACA
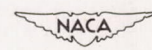
TABLE VII

EFFECT OF FLEXIBILITY OF SUPPORT ON CRITICAL LOAD

(a) Values of R_{cr} as a function of β

β \ λ_1	1.0	1.2	1.4	1.6	1.8	2.0	2.2	2.4	2.6	3.0	3.5	4.0
1.0	1.000	1.312	1.762	2.350	3.080	4.000	5.096	6.380	7.584	9.708	12.12	14.39
.95	-----	1.288	1.716	2.277	2.983	3.850	4.895	6.135	7.391	9.564	12.01	14.30
.90	-----	1.265	1.671	2.204	2.876	3.701	4.694	5.873	7.166	9.402	11.88	14.20
.80	-----	1.226	1.584	2.062	2.664	3.404	4.295	5.349	6.584	9.000	11.58	13.95
.70	-----	1.200	1.504	1.924	2.457	3.155	3.897	4.829	5.917	8.439	11.17	13.62
.60	-----	-----	1.437	1.795	2.256	2.823	3.505	4.312	5.255	7.587	10.59	13.16
.50	-----	-----	-----	1.681	2.066	2.544	3.121	3.803	4.598	6.565	9.686	12.48

(b) Solution of equation (71)
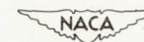
β	$(\lambda_1)_0$
1.0	2.345
.95	2.406
.90	2.471
.80	2.622
.70	2.803
.60	3.028
.50	3.317

TABLE VIII

VALUES OF R_{cr} FOR A SINUSOIDAL ARCH WITH A CENTRAL

ELASTIC SUPPORT AND $q = q_0 \sin \frac{\pi x}{L}$

λ_1 \ μ	0.5	1.0	1.5	2.0	3.0
1.42	2.82	No solution in this			
1.60	3.34				
1.74	3.87	5.10	region		
1.80	4.11	5.32			
2.00	5.06	6.25	7.61	9.28	12.46
2.20	6.21	7.40	8.54	9.62	11.66
2.40	7.43	8.43	9.38	10.29	12.00
3.00	10.45	11.17	11.84	12.49	13.70
3.50	17.73	13.32	13.87	14.40	16.40
4.00	14.92	15.42	15.89	16.34	17.20
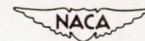
TABLE IX

THEORETICAL AND EXPERIMENTAL DATA

Specimen (1)	Length (in.)	Width (in.)	Thickness (in.)	λ_1	λ_2	λ_3	Buckling load (lb)	$(R_{cr})_{exp}$	$\dfrac{(R_{cr})_{exp}}{(R_{cr})_{class}}$
1	18	0.500	0.249	3.78	0.0138	0.136	82.7	5.19	0.880
2	$17\frac{15}{16}$	.495	.1885	9.12	.0055	.344	85.7	16.37	1.004
3	18	.500	.249	4.25	.0097	.146	107.0	6.72	.955
4	18	.499	.249	3.32	.0055	.114	73.7	4.63	.915
5	$17\frac{31}{32}$	.501	.249	2.63	.0417	.097	33.9	2.11	.653
6	$18\frac{1}{32}$	.493	.249	1.83	.0146	.063	16.2	1.04	.671
7	18	.502	.250	4.71	.0842	.159	98.5	6.07	.884
8	18	.502	.251	4.07	.0496	.167	94.4	5.72	.976
9	18	.504	.251	3.67	.0666	.164	80.0	4.83	.988
10	18	.505	.250	3.30	.0178	.123	60.4	3.70	.781
11	18	.502	.250	3.90	.0264	.126	96.7	5.95	1.003
12	18	.505	.250	5.31	.0015	.185	139.8	8.55	.926
13	18	.503	.250	5.07	.0957	.131	115.8	6.98	.925
14	$17\frac{31}{32}$	.502	.374	1.86	.0076	.0582	83.3	1.02	.630
15	$17\frac{15}{16}$	.500	.375	1.67	.0170	.0610	73.0	.886	.703
16	$17\frac{31}{32}$	.501	.374	1.38	.0013	.0459	(2)	------	-----
17	$17\frac{15}{16}$	.501	.374	1.265	.0141	.0472	(2)	------	-----
18	$17\frac{31}{32}$	.502	.374	2.44	.0015	.0850	157.3	1.93	.666
19	$17\frac{31}{32}$	.499	.374	2.08	.0043	.0707	129.9	1.60	.773
20	$17\frac{15}{16}$	.503	.374	1.34	.0244	.0500	(2)	------	-----
21	$17\frac{31}{32}$	.502	.374	2.43	.0112	.0883	176.9	2.16	.745
22	18	.501	.186	6.08	.0058	.237	48.2	9.70	.930
23	18	.499	.185	6.43	.0031	.236	53.6	10.96	.978
24	18	.500	.185	7.23	.0225	.257	62.5	12.89	1.031
25	18	.500	.186	9.15	.0007	.311	73.0	14.73	1.016

[1] Material: Specimens 1 to 13 and 22 to 25, 24S-T3; specimens 14 to 21, 75S-T6.
$E = 10.3 \times 10^7$ psi.

[2] Specimen did not buckle.

NACA
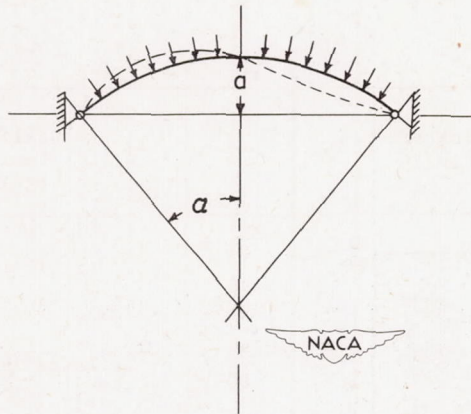
Figure 1.- Buckling mode for a high arch.
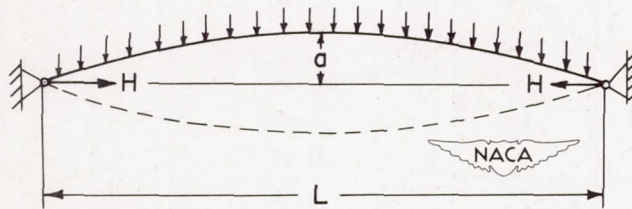
Figure 2.- Possible buckling mode for a low arch.
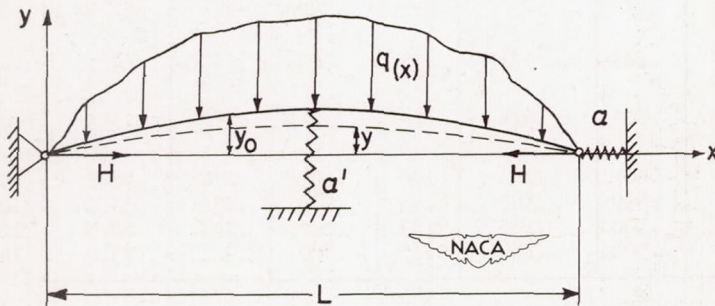
Figure 3.- Coordinate system.
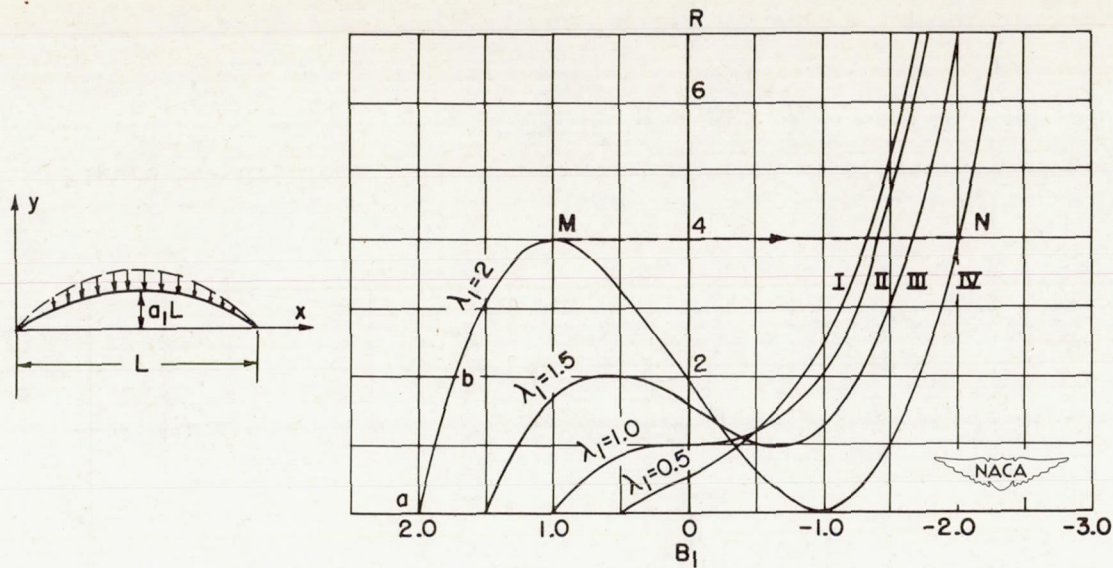
Figure 4.- Relation between B_1 and R for symmetrical buckling of a sinusoidal arch under a sinusoidal load.
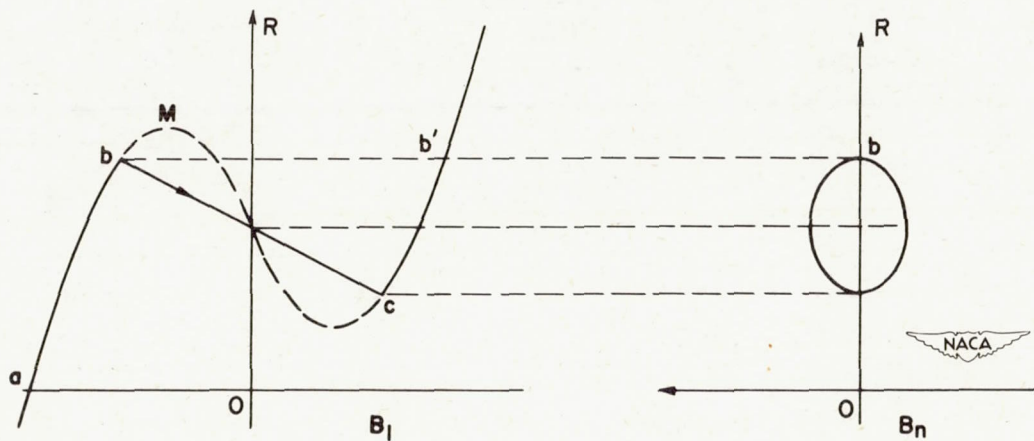
Figure 5.- Relations between B_1, B_n, and R for a sinusoidal arch which buckles in the -nth mode.
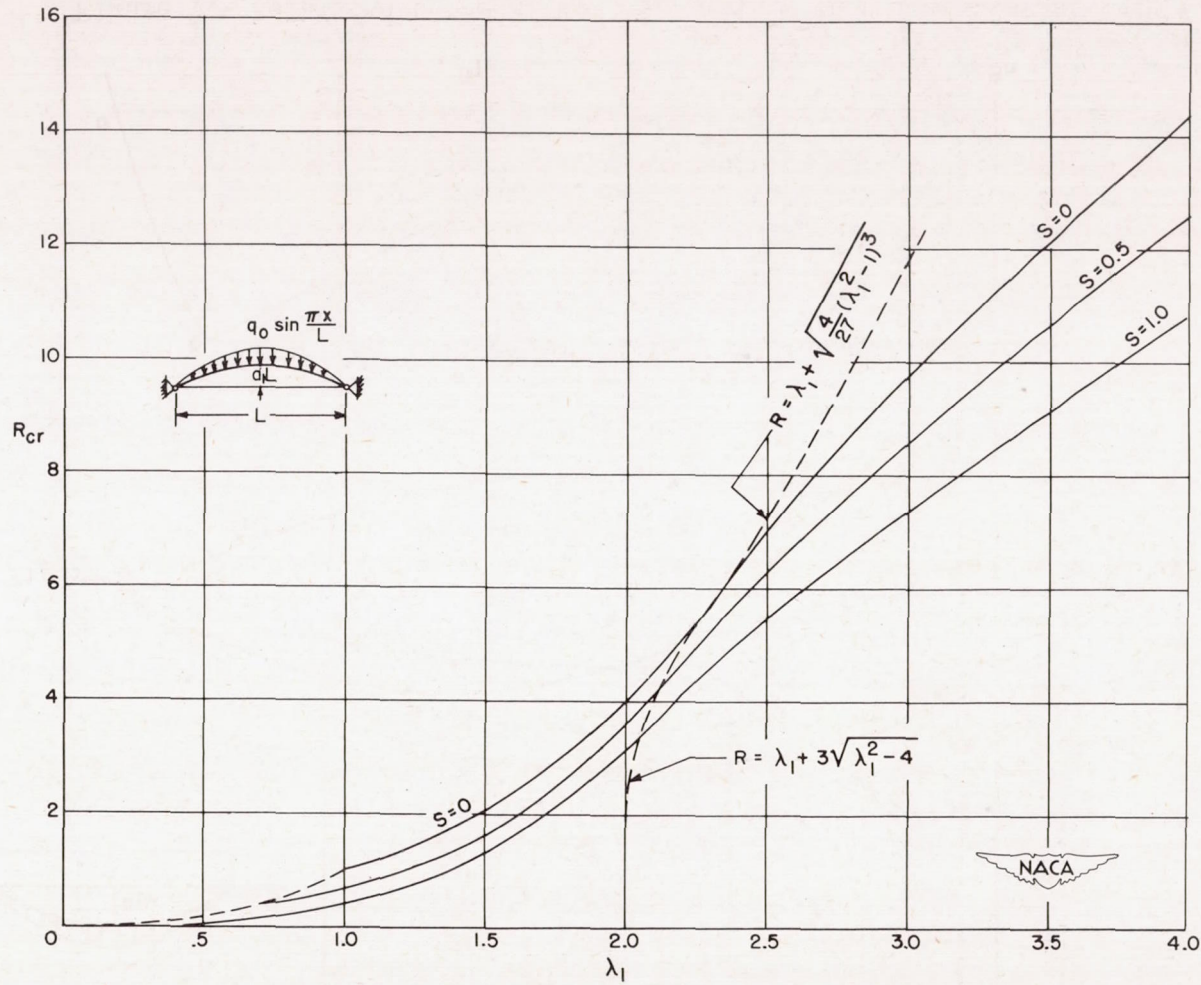
Figure 6.- Critical load on a sinusoidal arch as a function of arch rise.

$$\lambda_1 = \frac{a_1 L}{2}\sqrt{\frac{A}{I}}; \quad R = \frac{q_0 L^4}{2\pi^4 EI}\sqrt{\frac{A}{I}}.$$

Figure 7.- Deformation history of a sinusoidal arch.
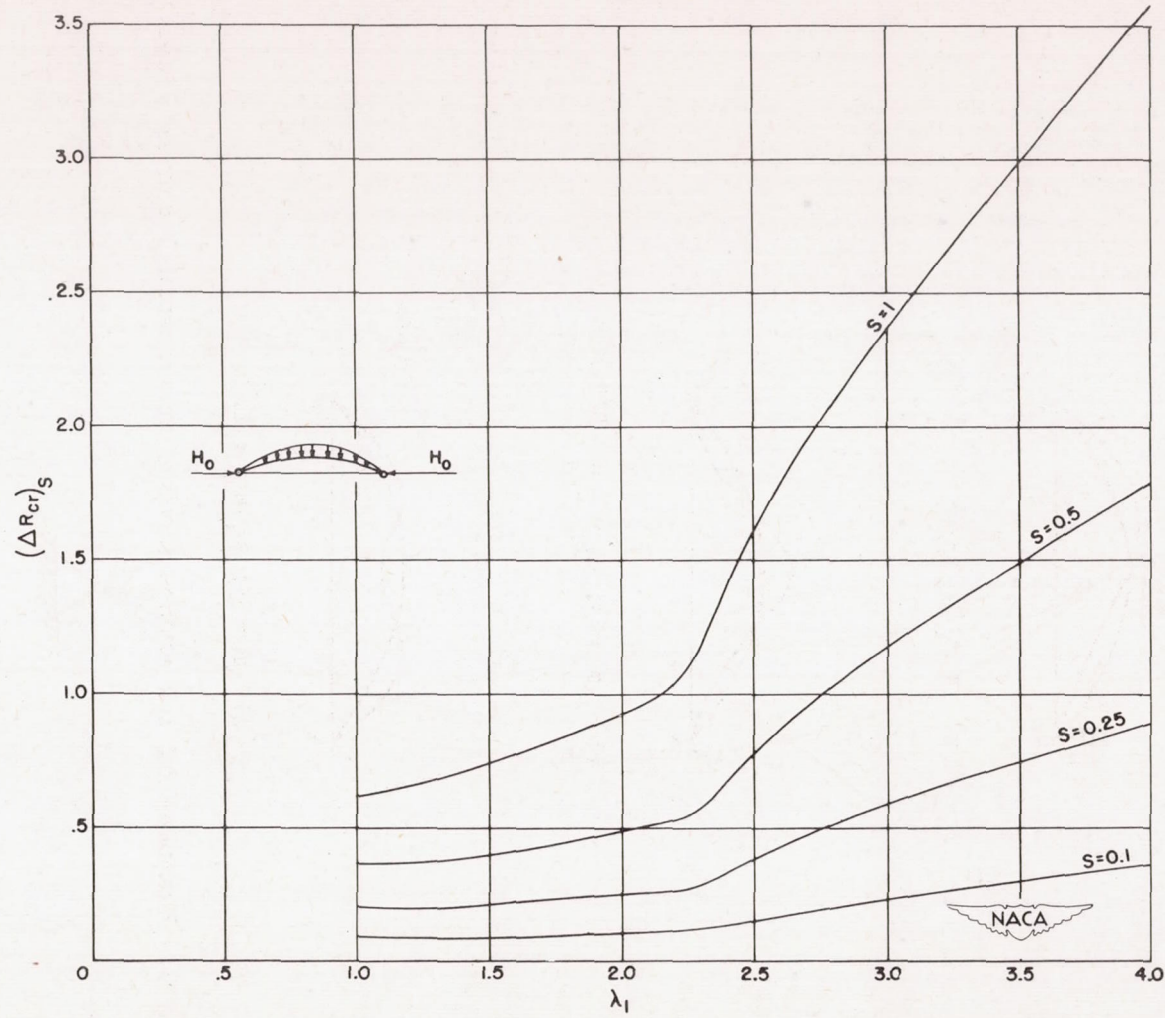
Figure 8.- Change of critical load due to initial thrust H_O.

$$(\Delta R_{cr})_S = (R_{cr})_{S=0} - (R_{cr})_{S=S}; \quad S = H_O L^2 / \pi^2 EI.$$
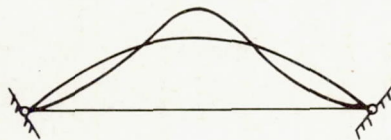
(a) $m = 2$; $a_2/a_1 = -1/3$.

(b) $m = 3$; $a_3/a_1 = -1/3$.
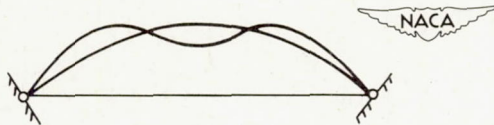
(c) $m = 3$; $a_3/a_1 = 1/3$.

Figure 9.- Examples of low arches having nonsinusoidal center lines.
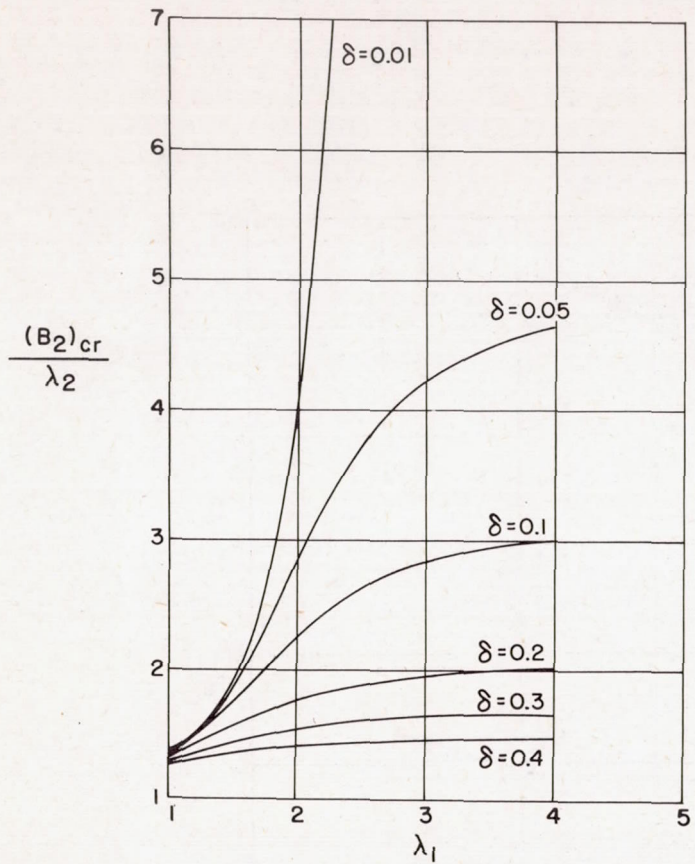
(a) Ratio of $(B_2)_{cr}/\lambda_2 = (b_2)_{cr}/a_2$.
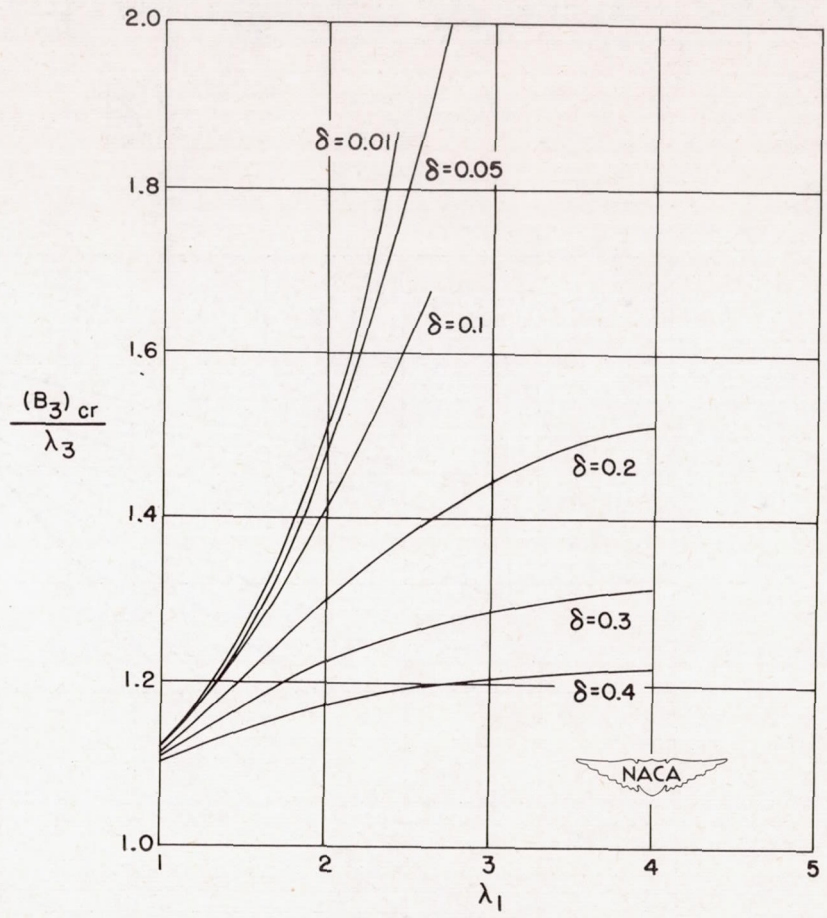
(b) Ratio of $(B_3)_{cr}/\lambda_3 = (b_3)_{cr}/a_3$.

Figure 10.- Solution of equation (40) for $m = 2$ and $m = 3$.
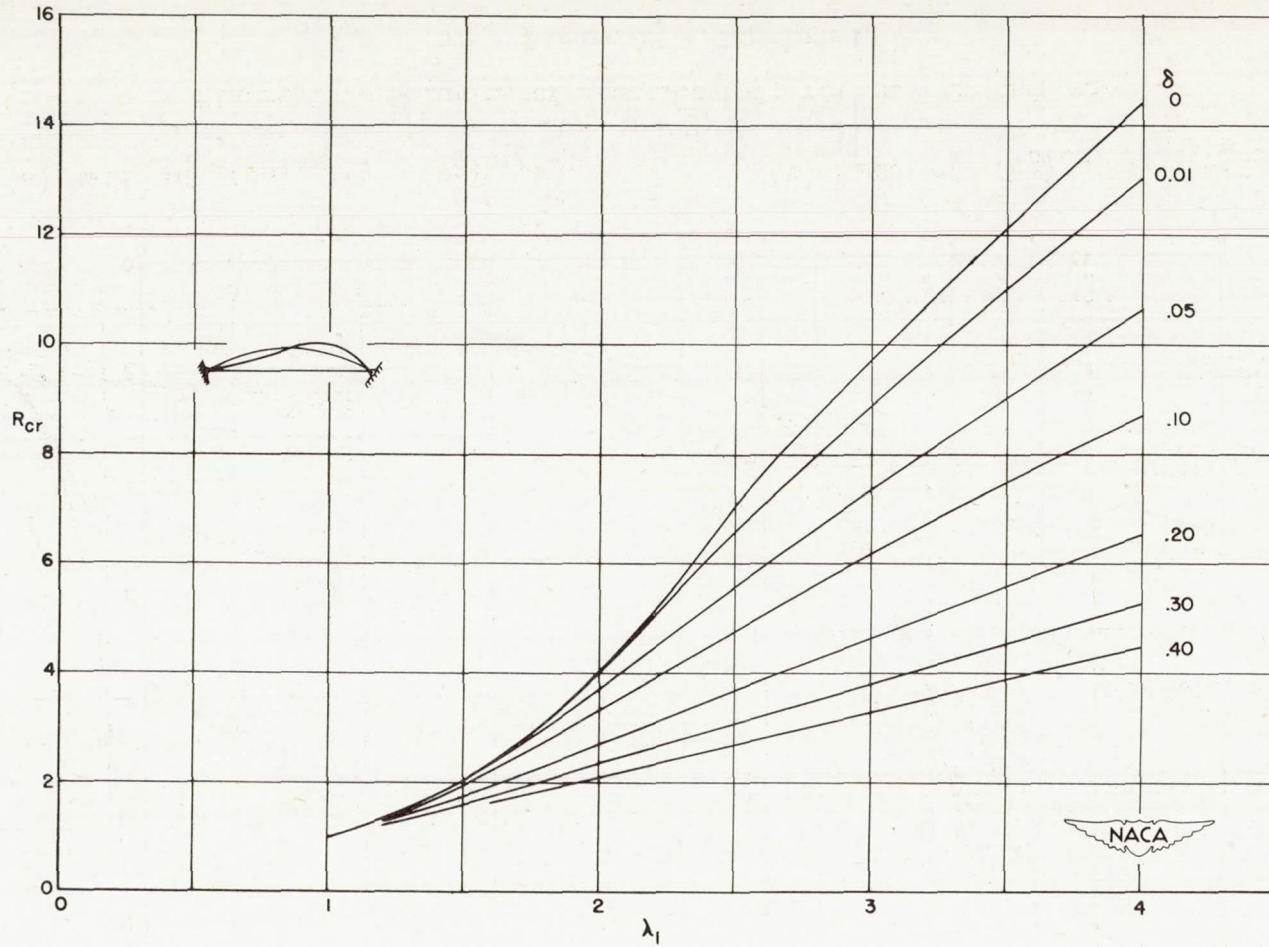
(a) $m = 2$; $\delta = \left| \dfrac{a_2}{a_1} \right|$.

Figure 11.- R_{cr} (sinusoidal) for arch forms $\dfrac{y_0}{L} = a_1 \sin \dfrac{\pi x}{L} + a_m \sin \dfrac{m \pi x}{L}$ with $m = 2$ and 3.
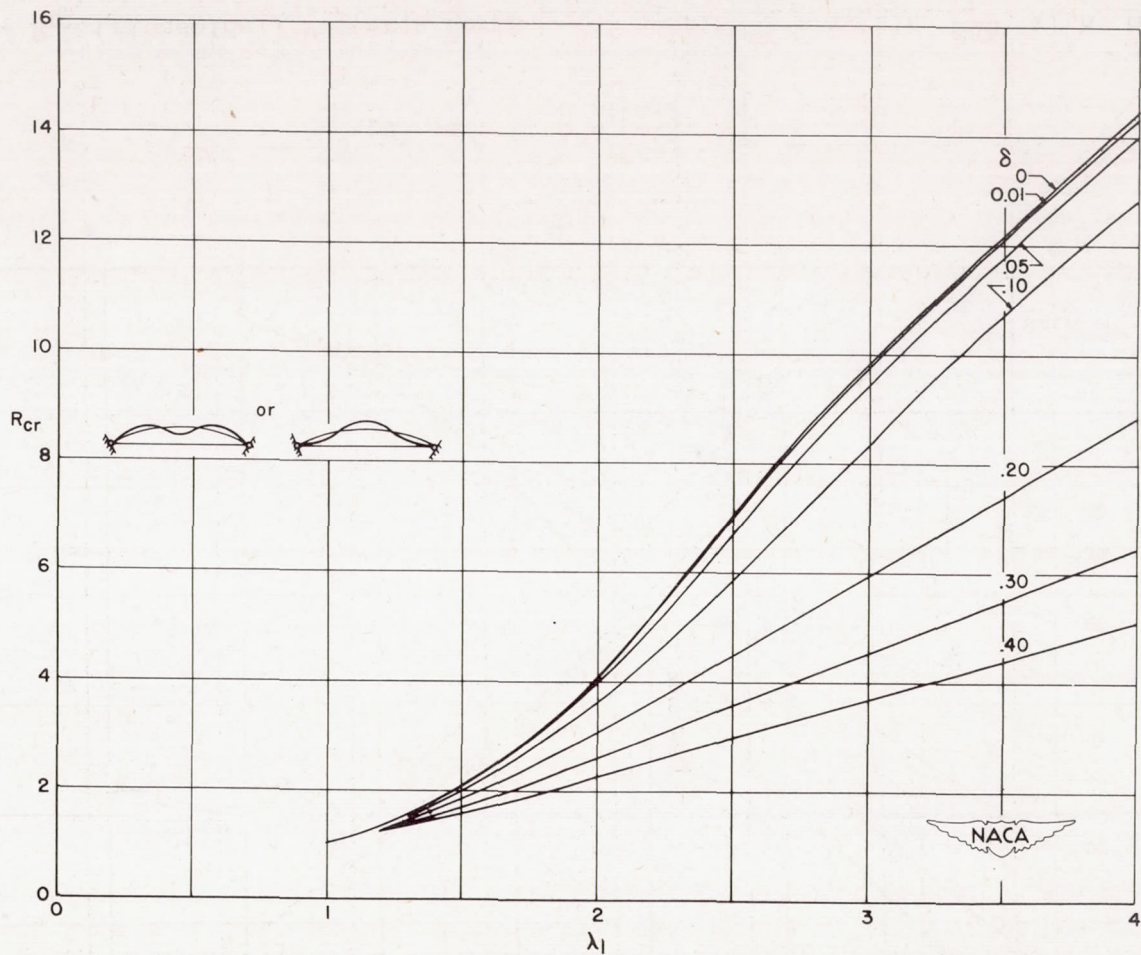
(b) $m = 3$; $\delta = \left| \dfrac{a_3}{a_1} \right|$.

Figure 11.- Concluded.
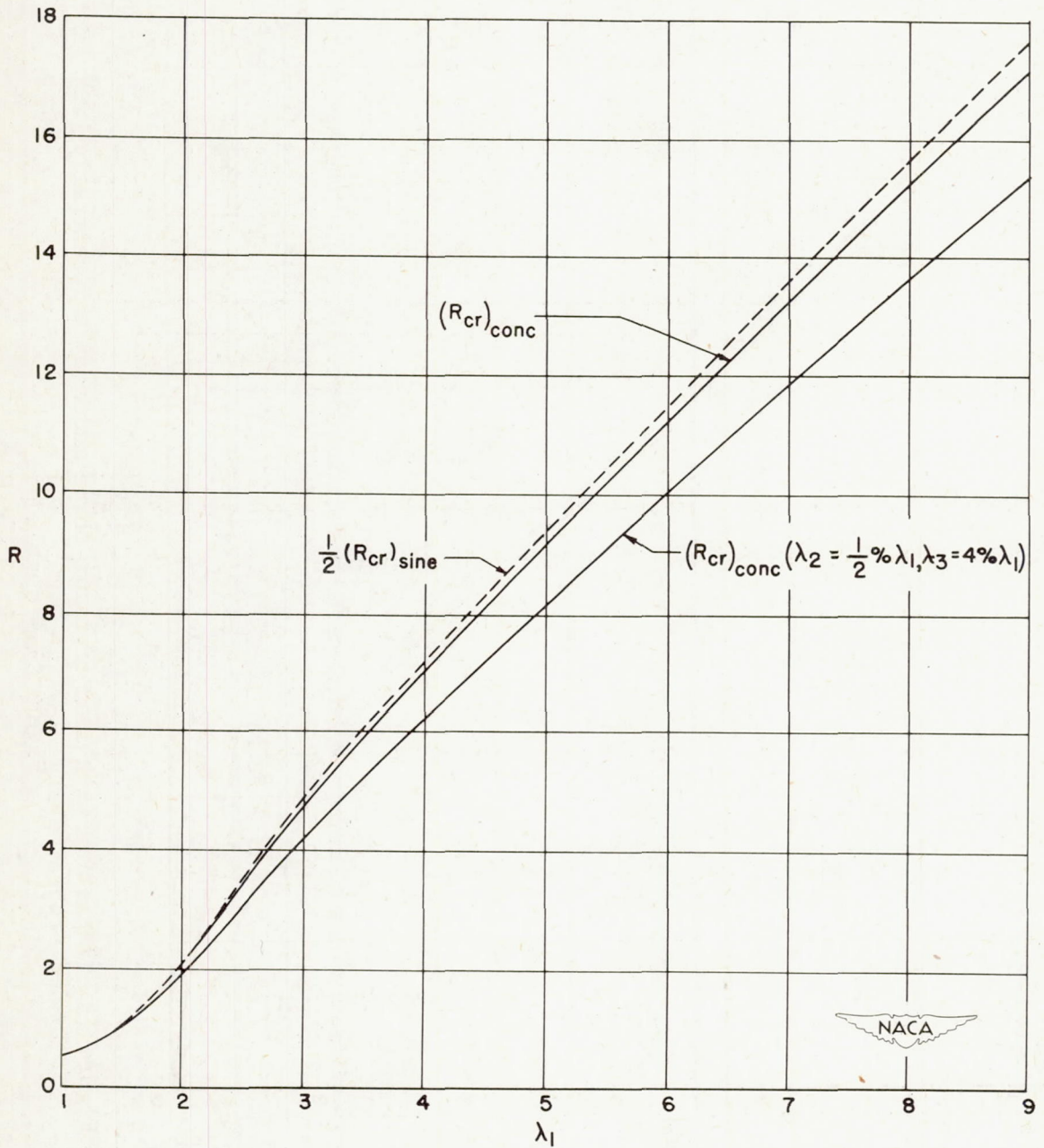
Figure 12.- R_{cr} for arches under a concentrated central load.
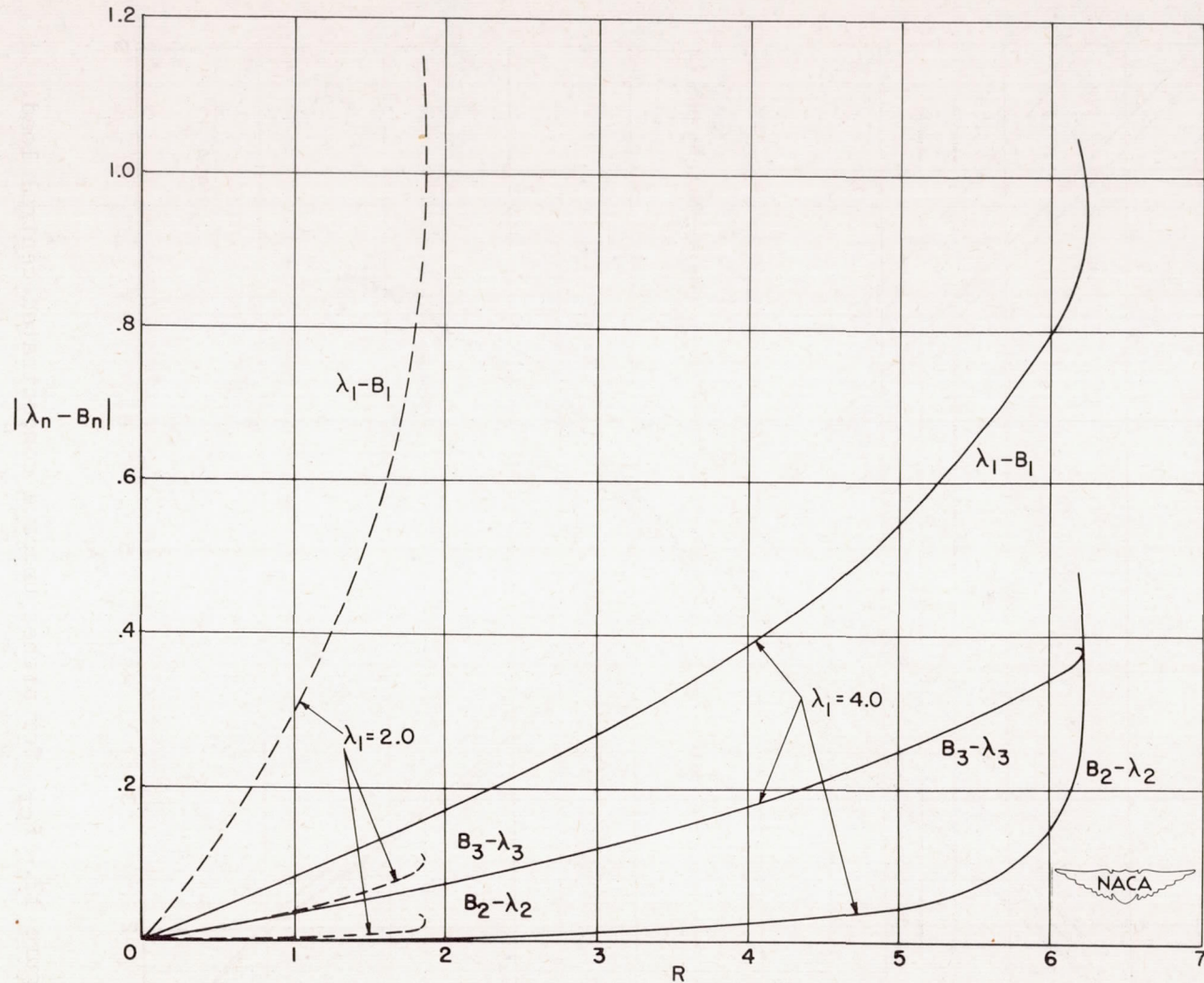
Figure 13.- Variation with load of first three modes of two centrally loaded arches having $\lambda_2/\lambda_1 = 0.005$ and $\lambda_3/\lambda_1 = 0.040$.
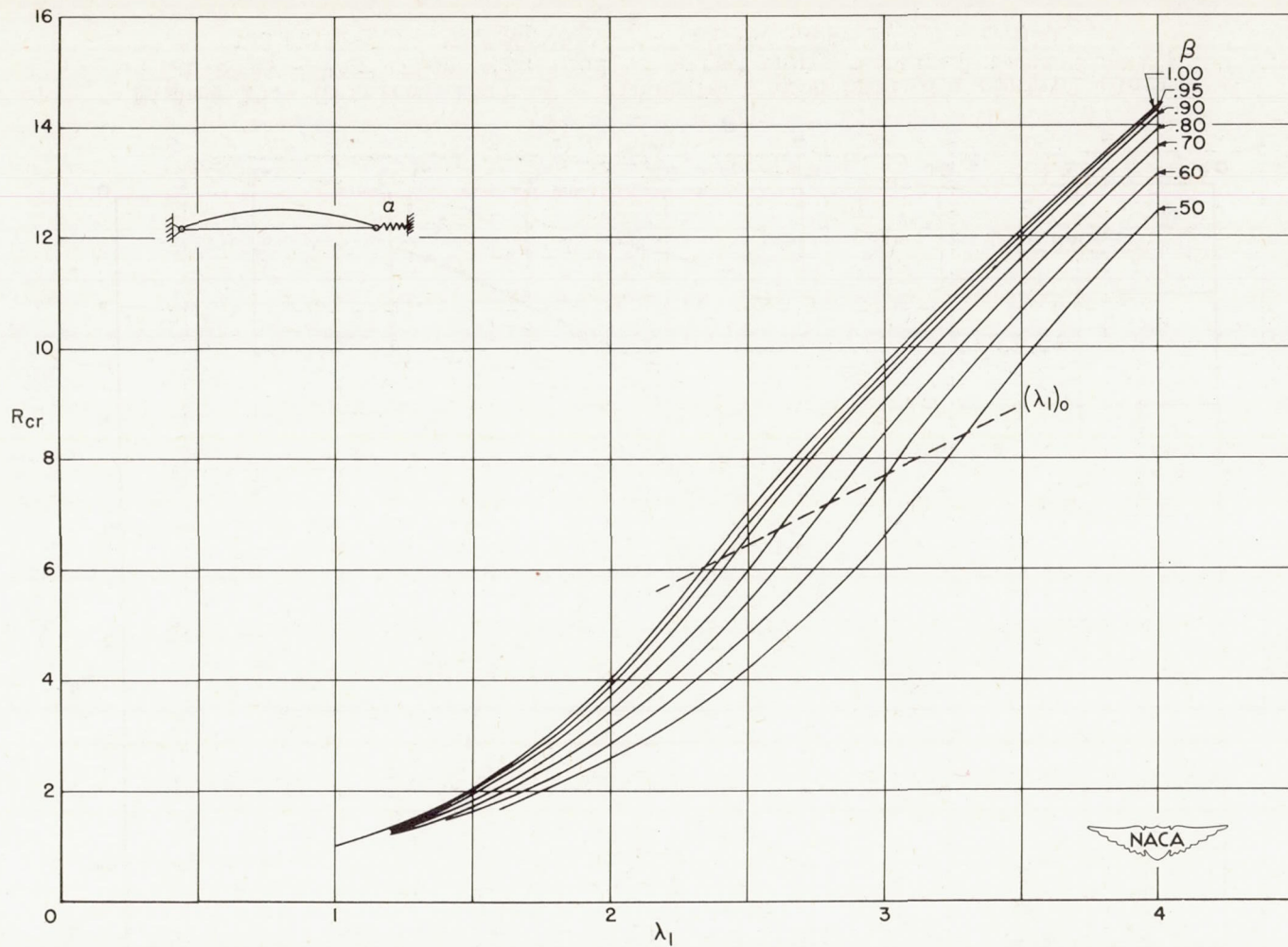
Figure 14.- Effect of support flexibility on critical load. $\beta = \dfrac{\alpha}{\alpha + \dfrac{EA}{L}}$.
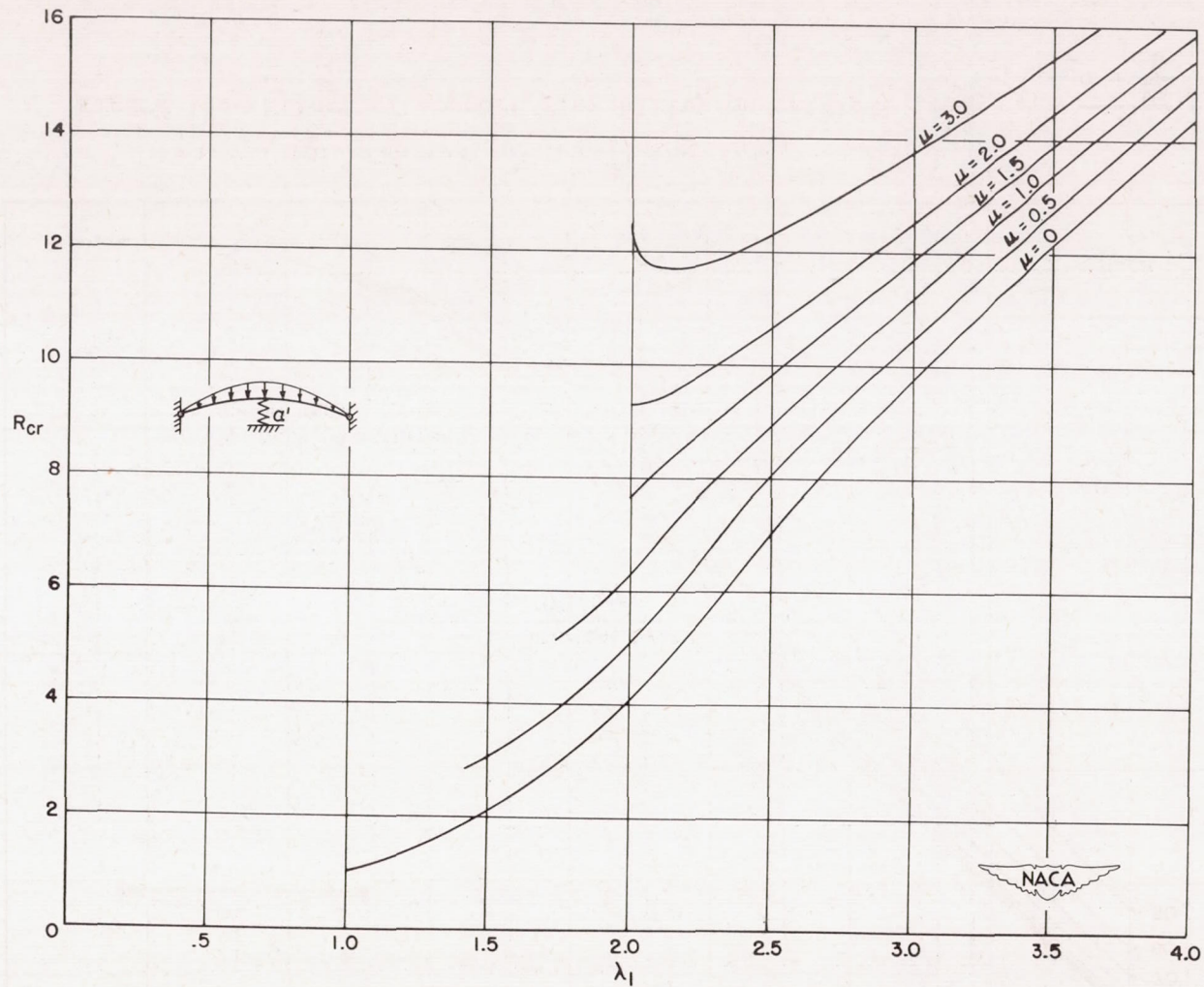
Figure 15.- Critical load of a sinusoidal arch having a central elastic support. $\mu = 2L^3\alpha'/\pi^4 EI$.
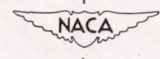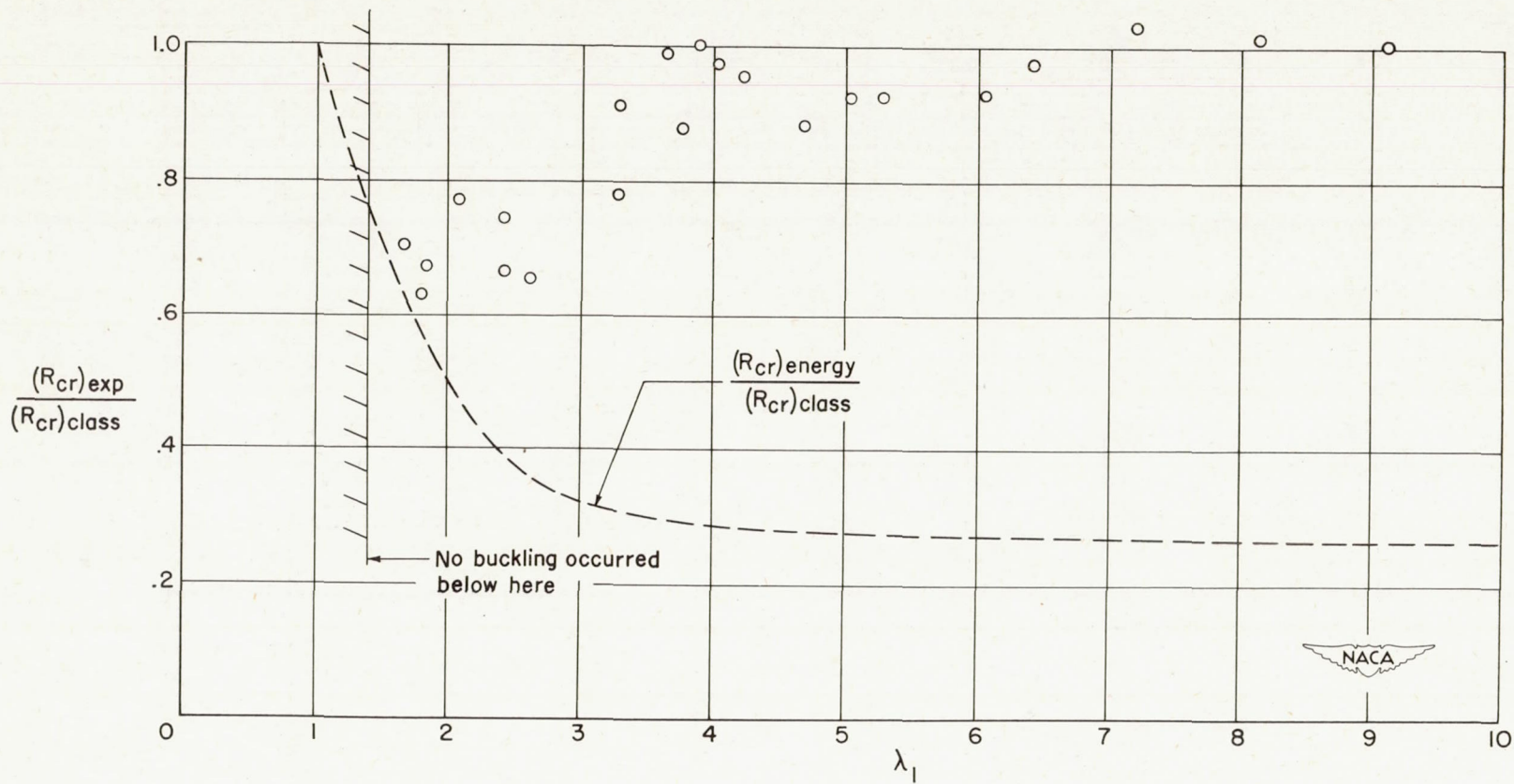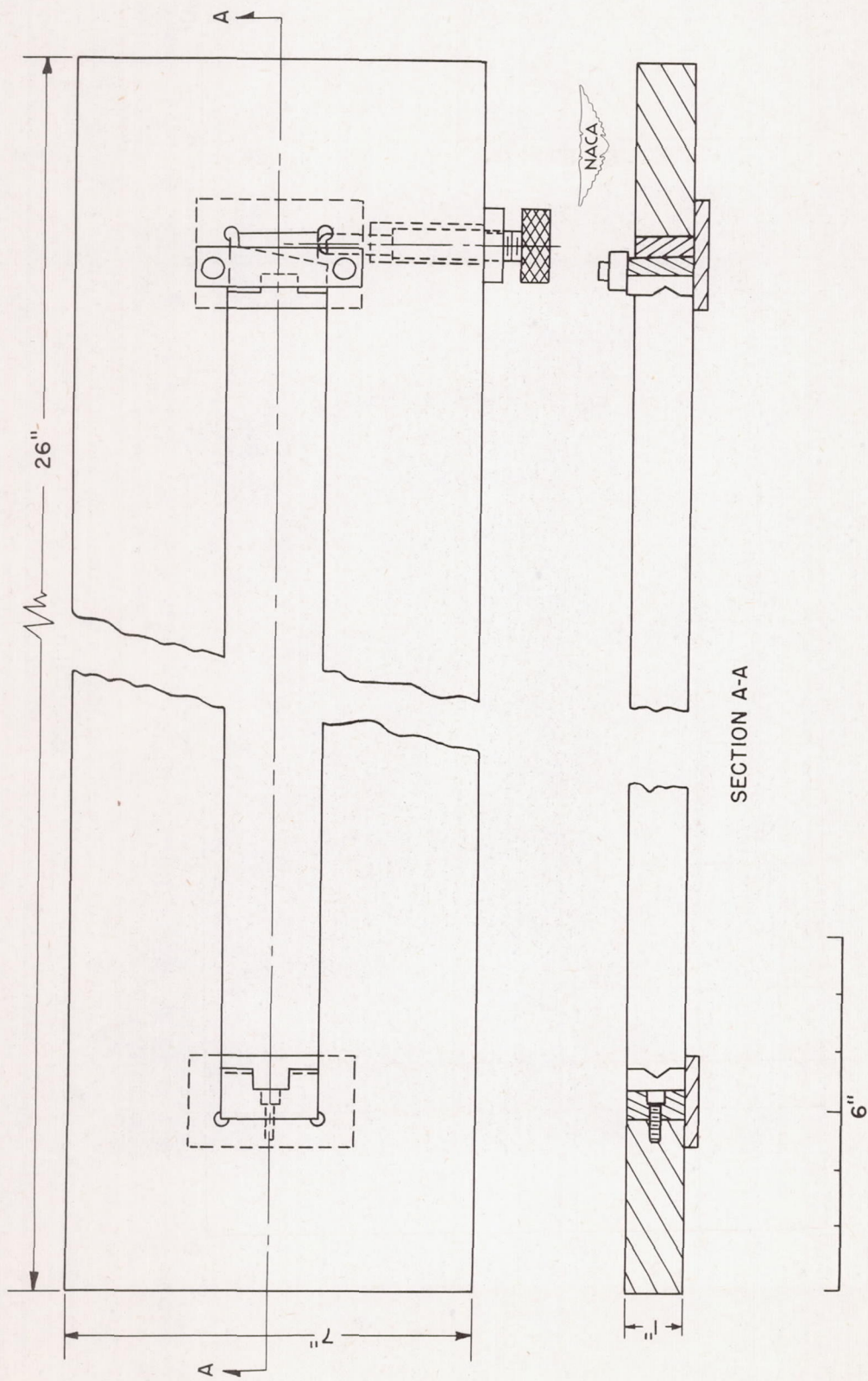
Figure 16.- Theoretical and experimental results.
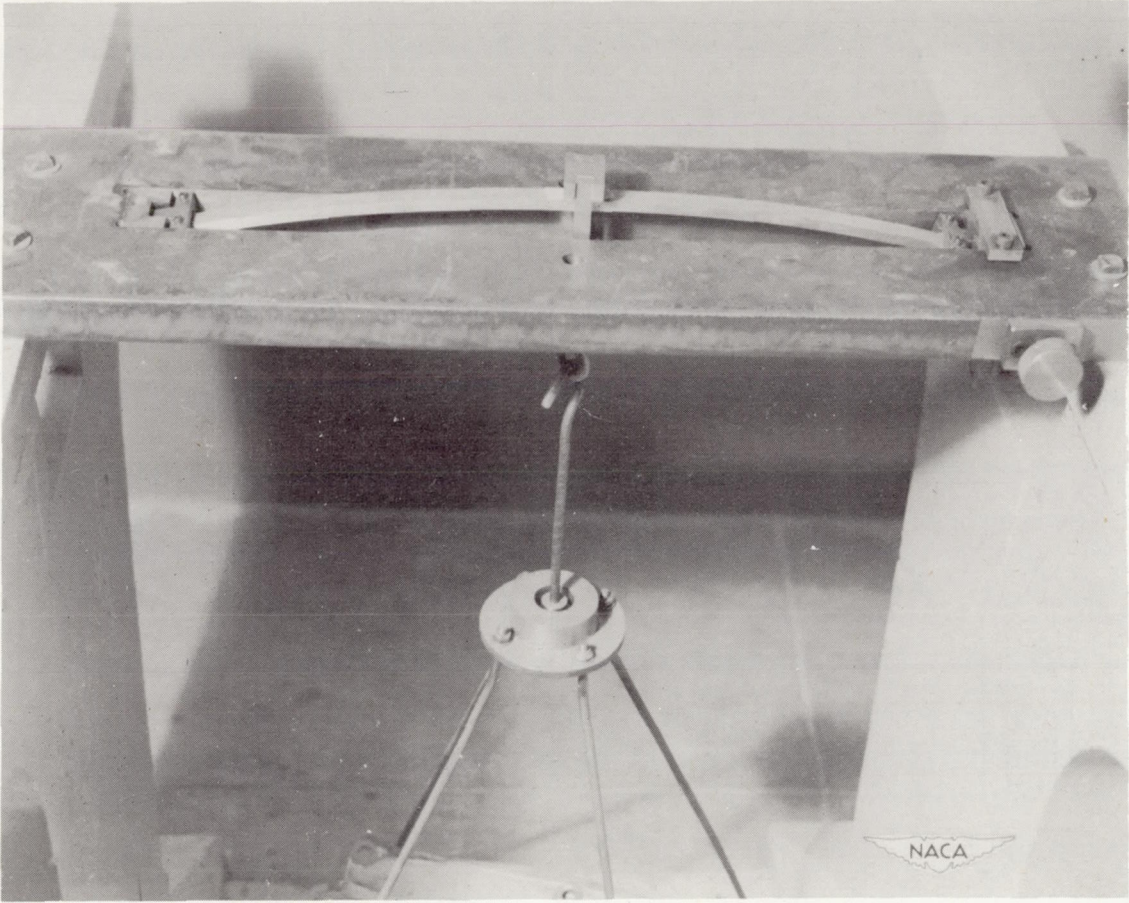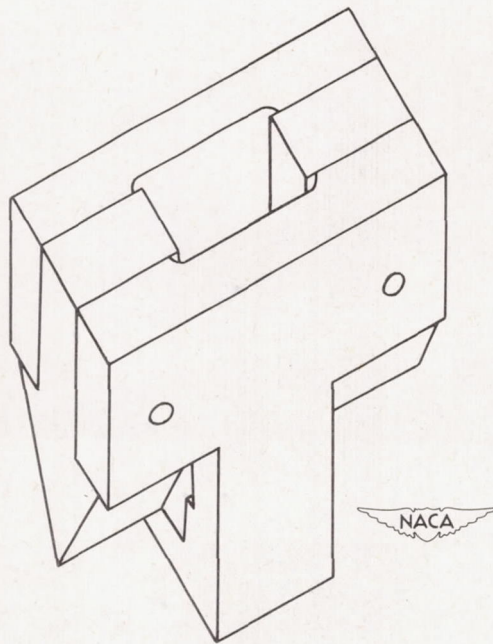
Figure 17.- Testing jig.

Figure 18.- Testing apparatus with specimen in place.

Figure 19.- Knife-edge fitting.